LHC as Neutrino-Ion Collider: FPF Case Studies

Tanjona R. Rabemananjara

Low-x 2023 - September 3-8, 2023

Leros Island, Greece

OUTLINE OF THE TALK:

1. Introduction & Motivations
2. Physics Potential of FPF
3. Hadron Substructure with LHC Neutrinos
4. Neutrino Structure Functions from GeV to EeV
5. Conclusions

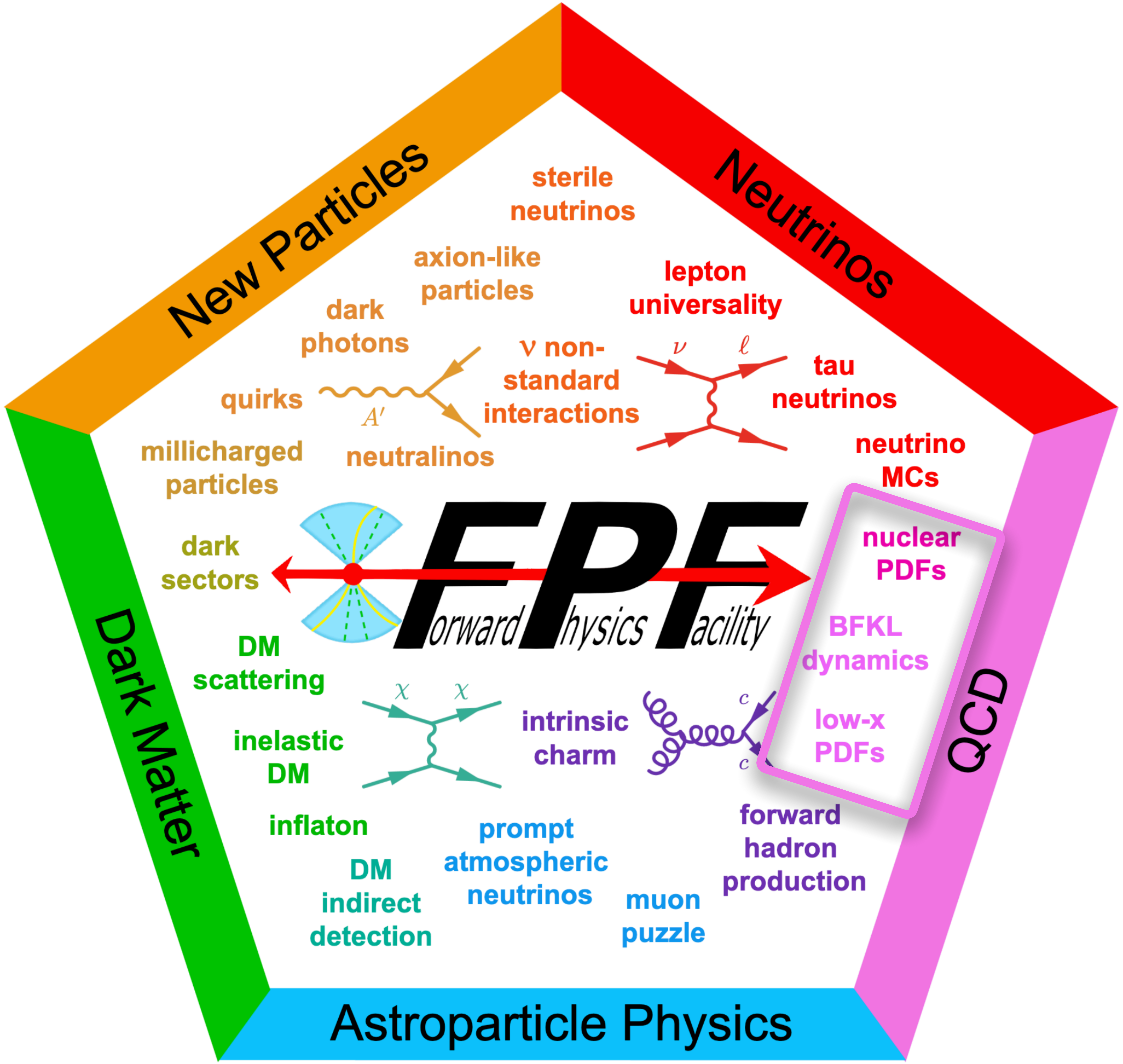

New Particles

Neutrinos

QCD

Astroparticle Physics

Dark Matter

sterile neutrinos

axion-like particles

dark photons

quirks

millicharged particles

neutralinos

ν non-standard interactions

lepton universality

tau neutrinos

neutrino MCs

nuclear PDFs

BFKL dynamics

low-x PDFs

dark sectors

FPF

Forward Physics Facility

DM scattering

inelastic DM

intrinsic charm

inflaton

DM indirect detection

prompt atmospheric neutrinos

muon puzzle

forward hadron production

Introduction & Motivations

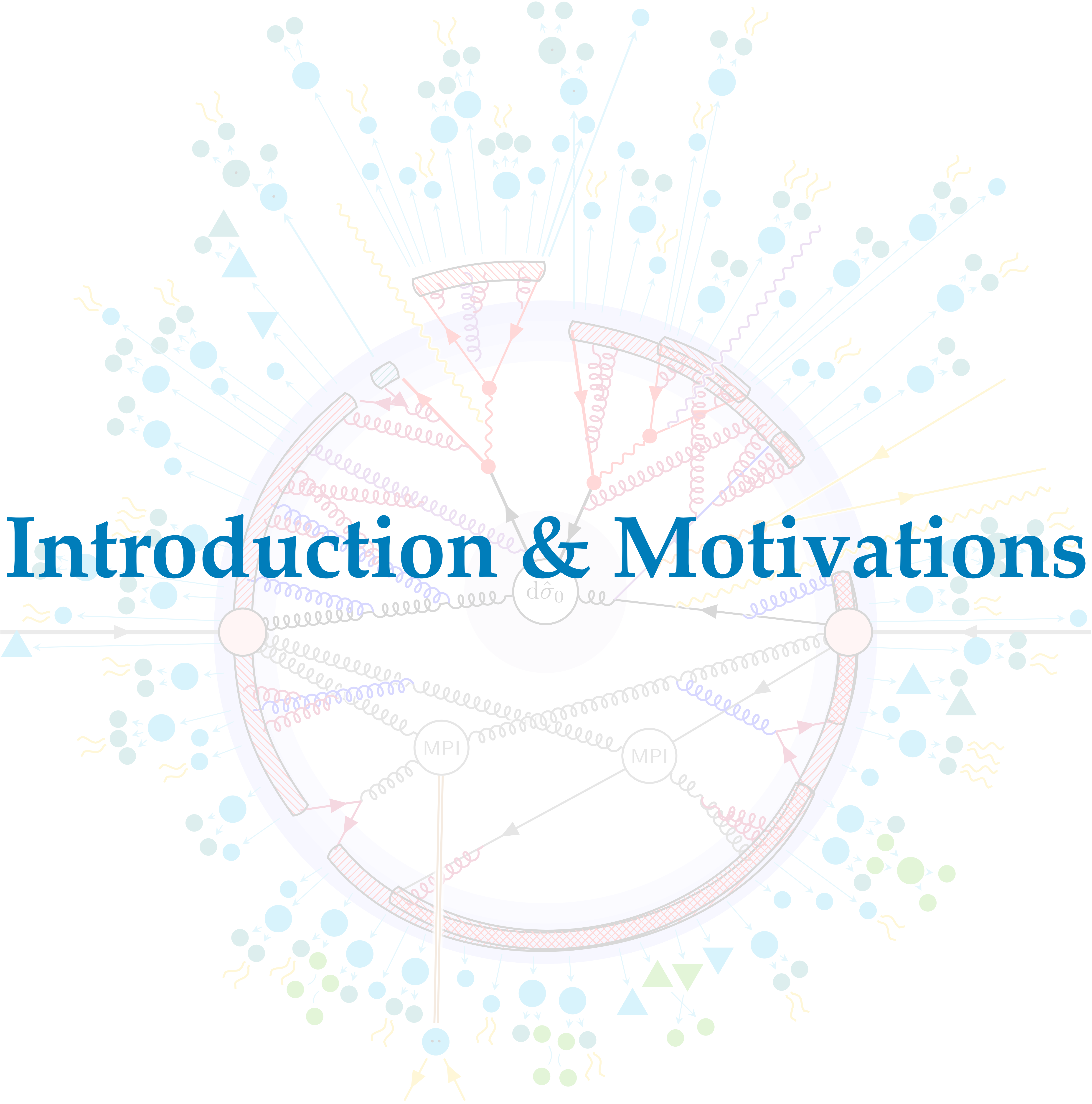

Introduction & Motivations

Main LHC detectors were designed to identify weak scale and heavier particles whose decay lie in central rapidity

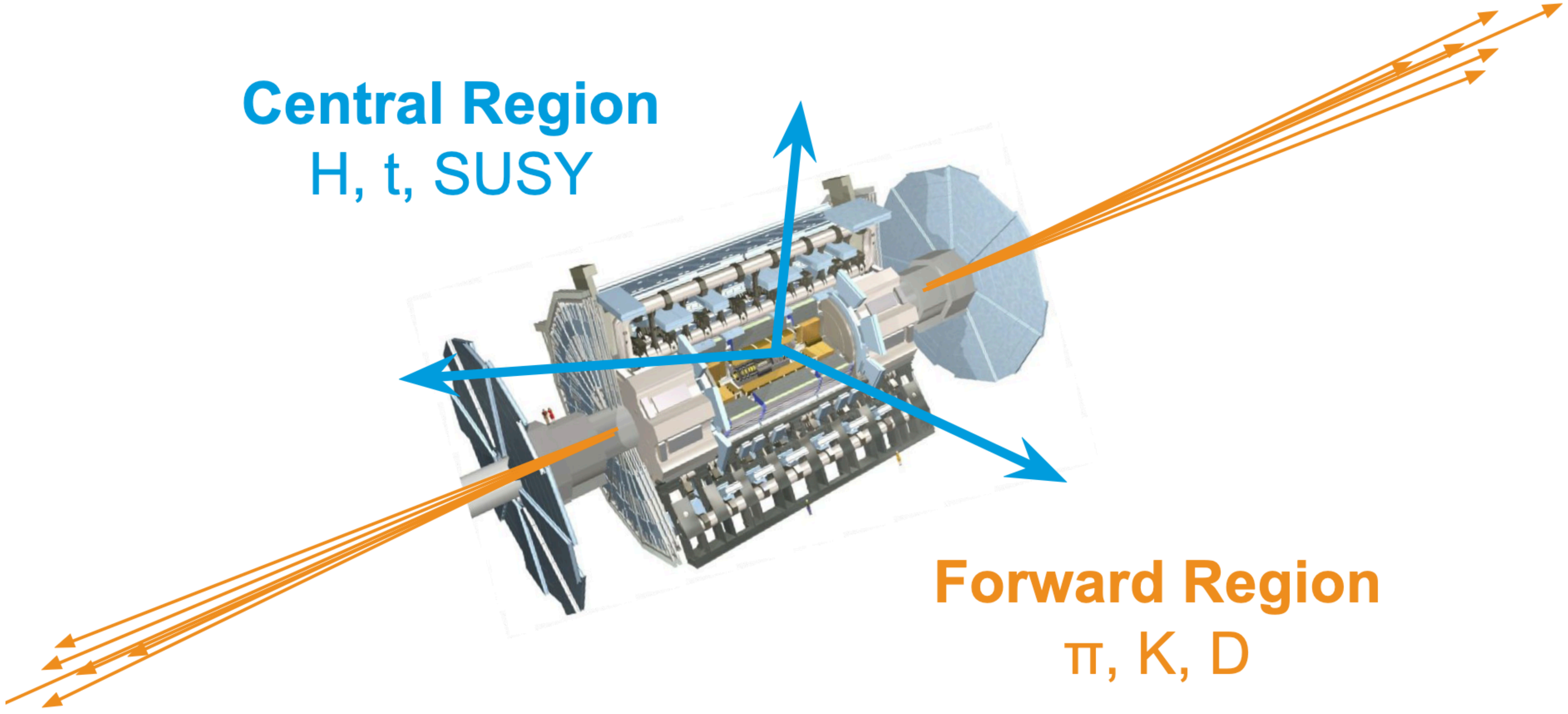

Central Region
H, t, SUSY

Forward Region
π, K, D

Introduction & Motivations

LHC produces an intense and strongly collimated beam of highly energetic particles in the forward direction.

These fluxes escape the detectors ⟺ Major Blind Spot of LHC

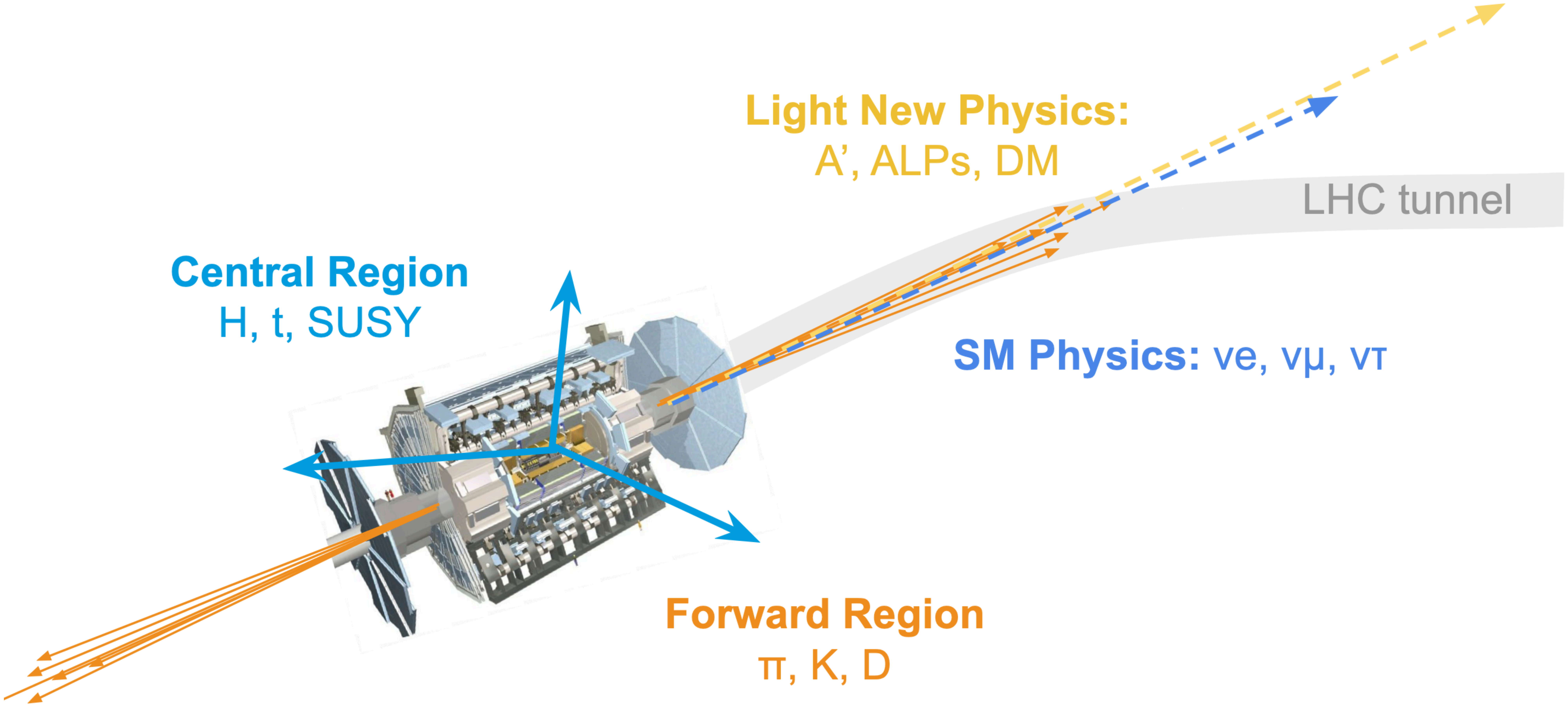

Introduction & Motivations: Far-Forward Detectors

Being able to detect most energetic human-made neutrinos would open new avenues.

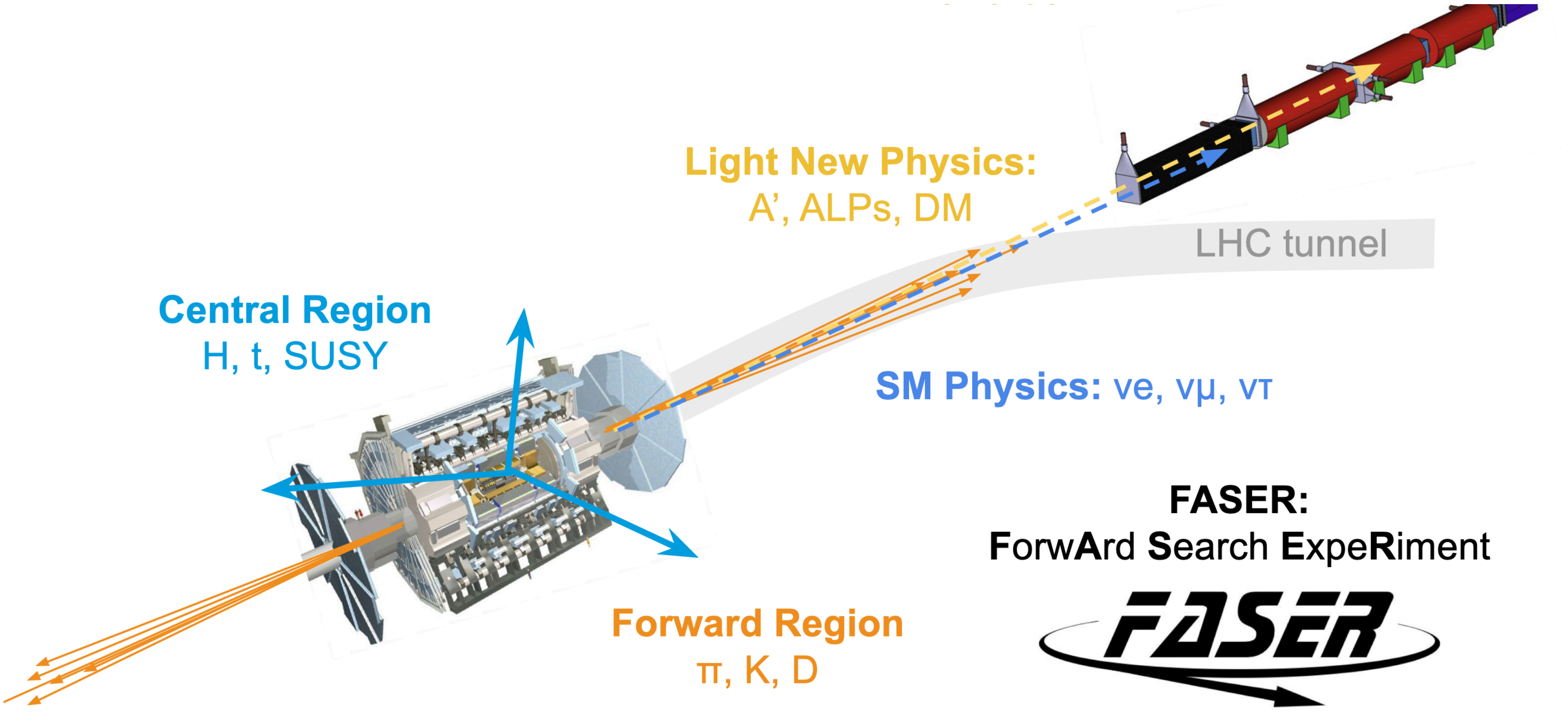

Light New Physics:
A', ALPs, DM

LHC tunnel

Central Region
H, t, SUSY

SM Physics: νe, $\nu \mu$, $\nu \tau$

Forward Region
π, K, D

FASER:
Forw**A**rd **S**earch **E**xpe**R**iment

FASER

Introduction & Motivations: Far-Forward Detectors

Two far-forward experiments have been operating at LHC since Run III and reported Evidence of LHC neutrinos

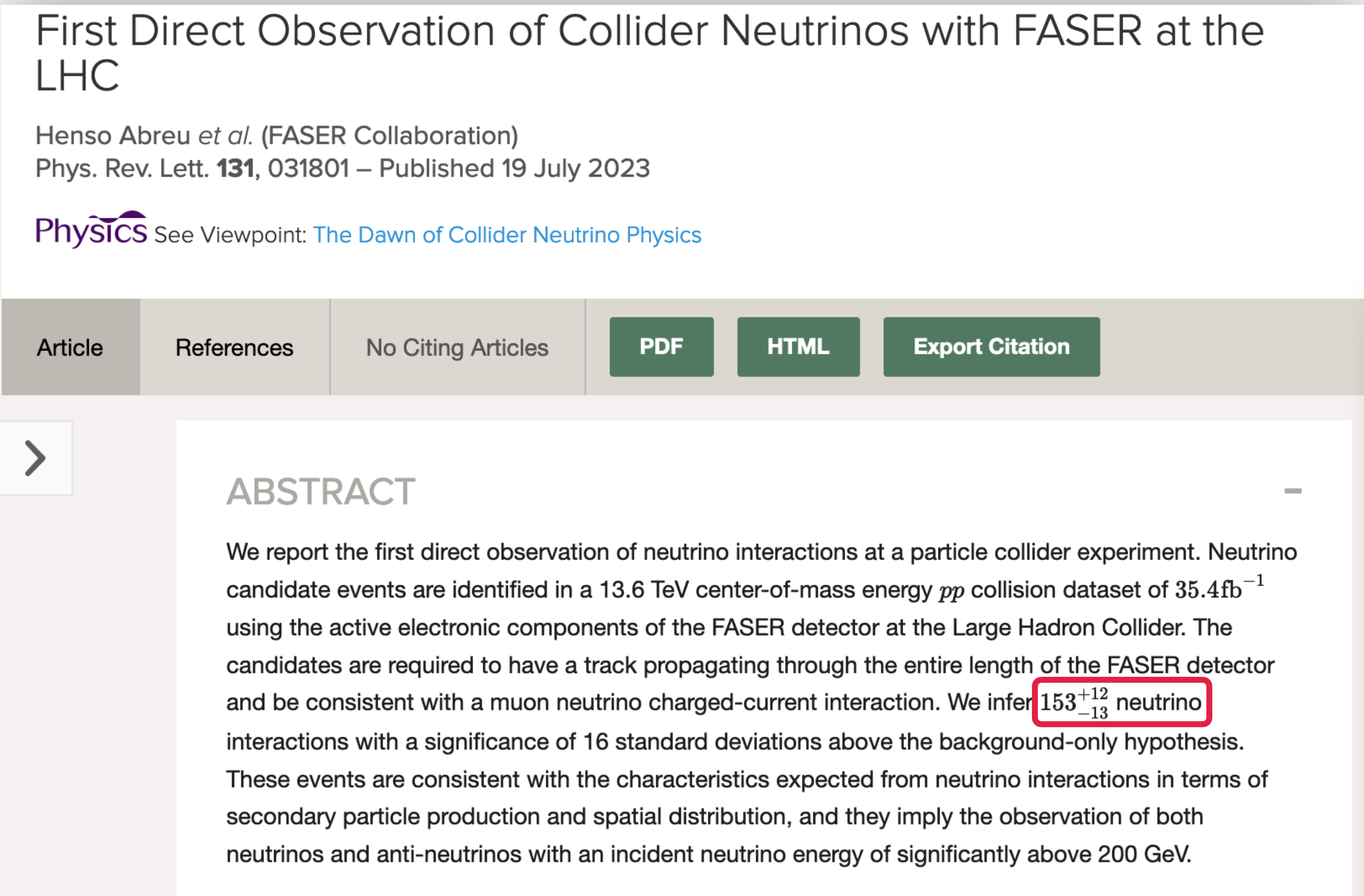

First Direct Observation of Collider Neutrinos with FASER at the LHC

Henso Abreu *et al.* (FASER Collaboration)
Phys. Rev. Lett. **131**, 031801 – Published 19 July 2023

Physics See Viewpoint: The Dawn of Collider Neutrino Physics

ABSTRACT

We report the first direct observation of neutrino interactions at a particle collider experiment. Neutrino candidate events are identified in a 13.6 TeV center-of-mass energy pp collision dataset of $35.4\,\mathrm{fb}^{-1}$ using the active electronic components of the FASER detector at the Large Hadron Collider. The candidates are required to have a track propagating through the entire length of the FASER detector and be consistent with a muon neutrino charged-current interaction. We infer 153^{+12}_{-13} neutrino interactions with a significance of 16 standard deviations above the background-only hypothesis. These events are consistent with the characteristics expected from neutrino interactions in terms of secondary particle production and spatial distribution, and they imply the observation of both neutrinos and anti-neutrinos with an incident neutrino energy of significantly above 200 GeV.

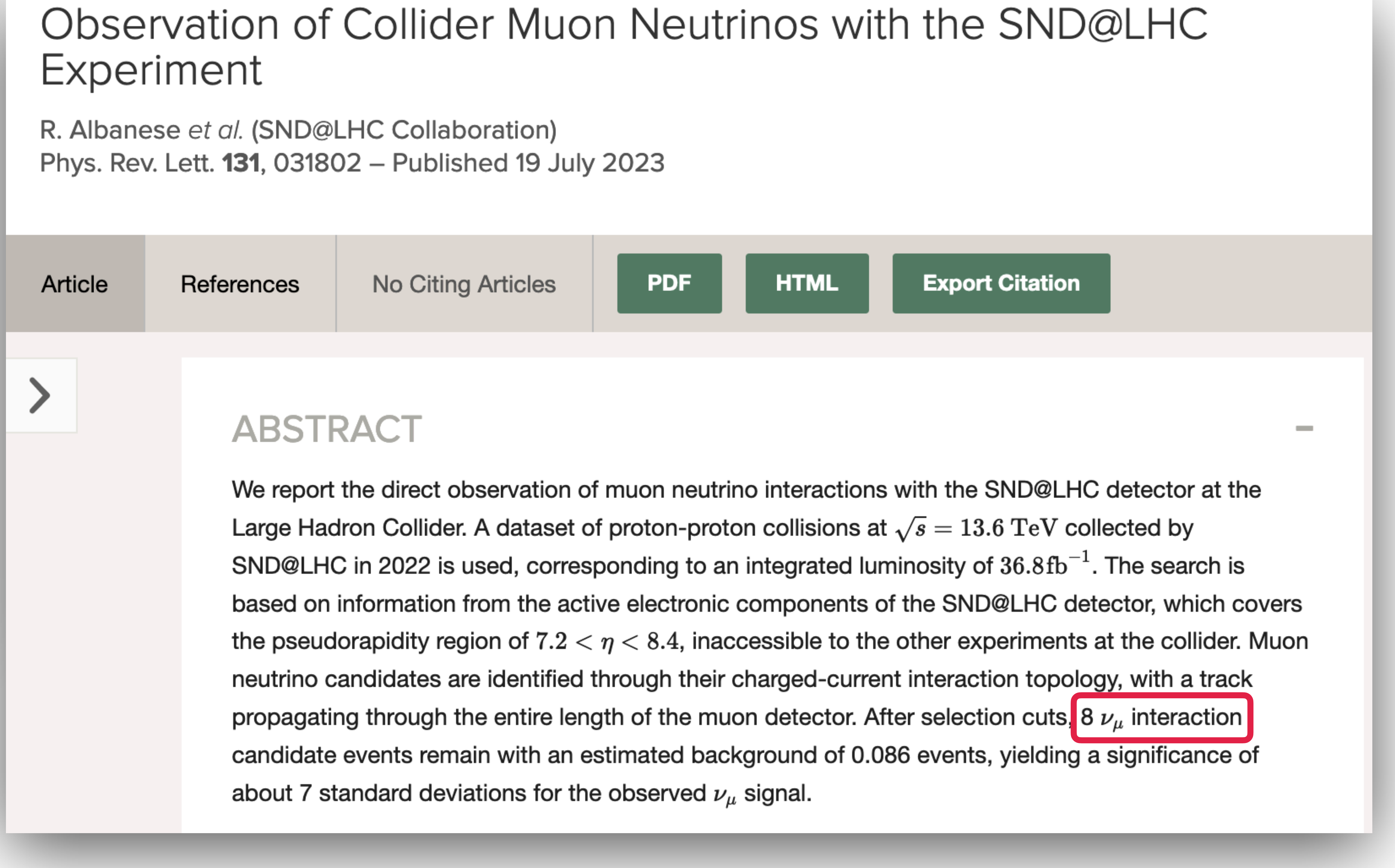

Observation of Collider Muon Neutrinos with the SND@LHC Experiment

R. Albanese *et al.* (SND@LHC Collaboration)
Phys. Rev. Lett. **131**, 031802 – Published 19 July 2023

ABSTRACT

We report the direct observation of muon neutrino interactions with the SND@LHC detector at the Large Hadron Collider. A dataset of proton-proton collisions at $\sqrt{s} = 13.6\,\mathrm{TeV}$ collected by SND@LHC in 2022 is used, corresponding to an integrated luminosity of $36.8\,\mathrm{fb}^{-1}$. The search is based on information from the active electronic components of the SND@LHC detector, which covers the pseudorapidity region of $7.2 < \eta < 8.4$, inaccessible to the other experiments at the collider. Muon neutrino candidates are identified through their charged-current interaction topology, with a track propagating through the entire length of the muon detector. After selection cuts, $8\ \nu_\mu$ interaction candidate events remain with an estimated background of 0.086 events, yielding a significance of about 7 standard deviations for the observed ν_μ signal.

Introduction & Motivations: Forward Physics Facility

A new proposed facility at CERN that will complement the far-forward experiments and Exploit the full potential of LHC far-forward physics

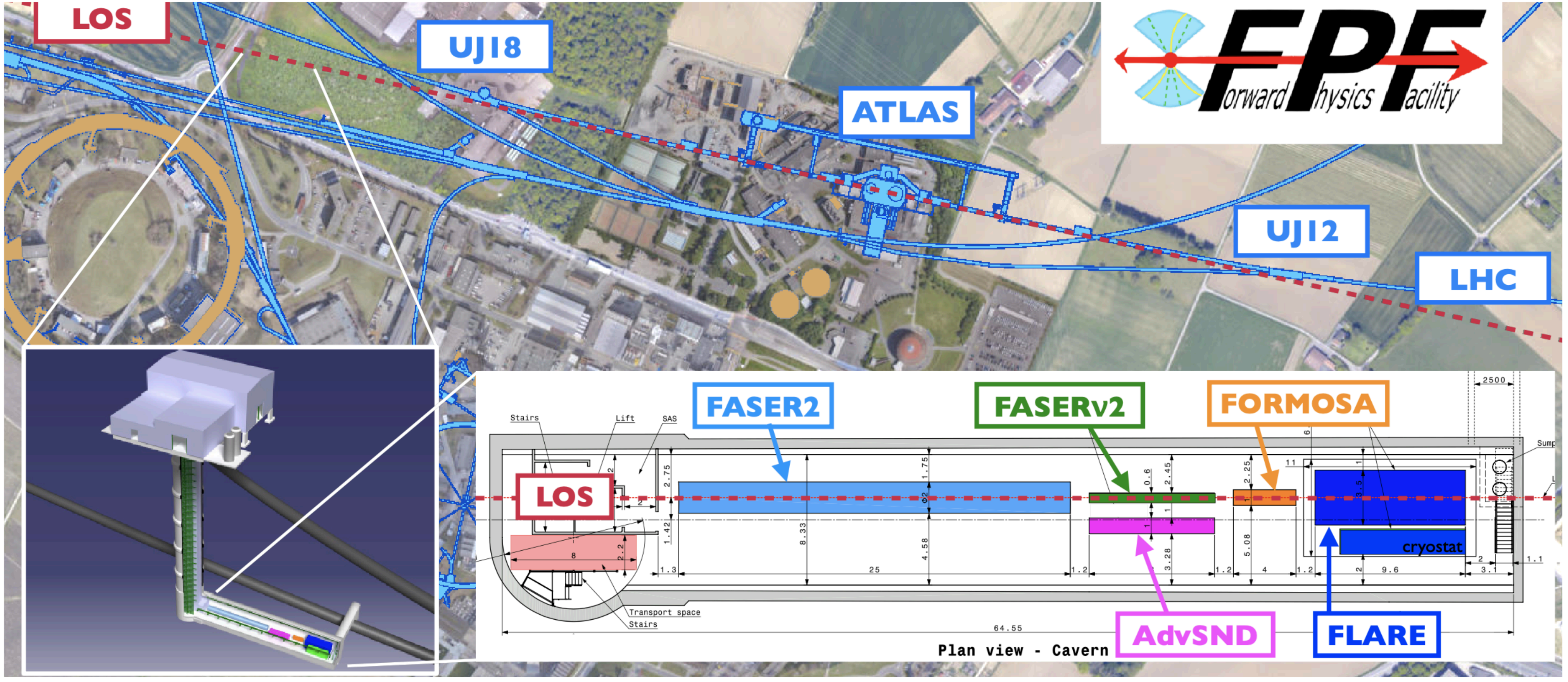

Introduction & Motivations: Forward Physics Facility

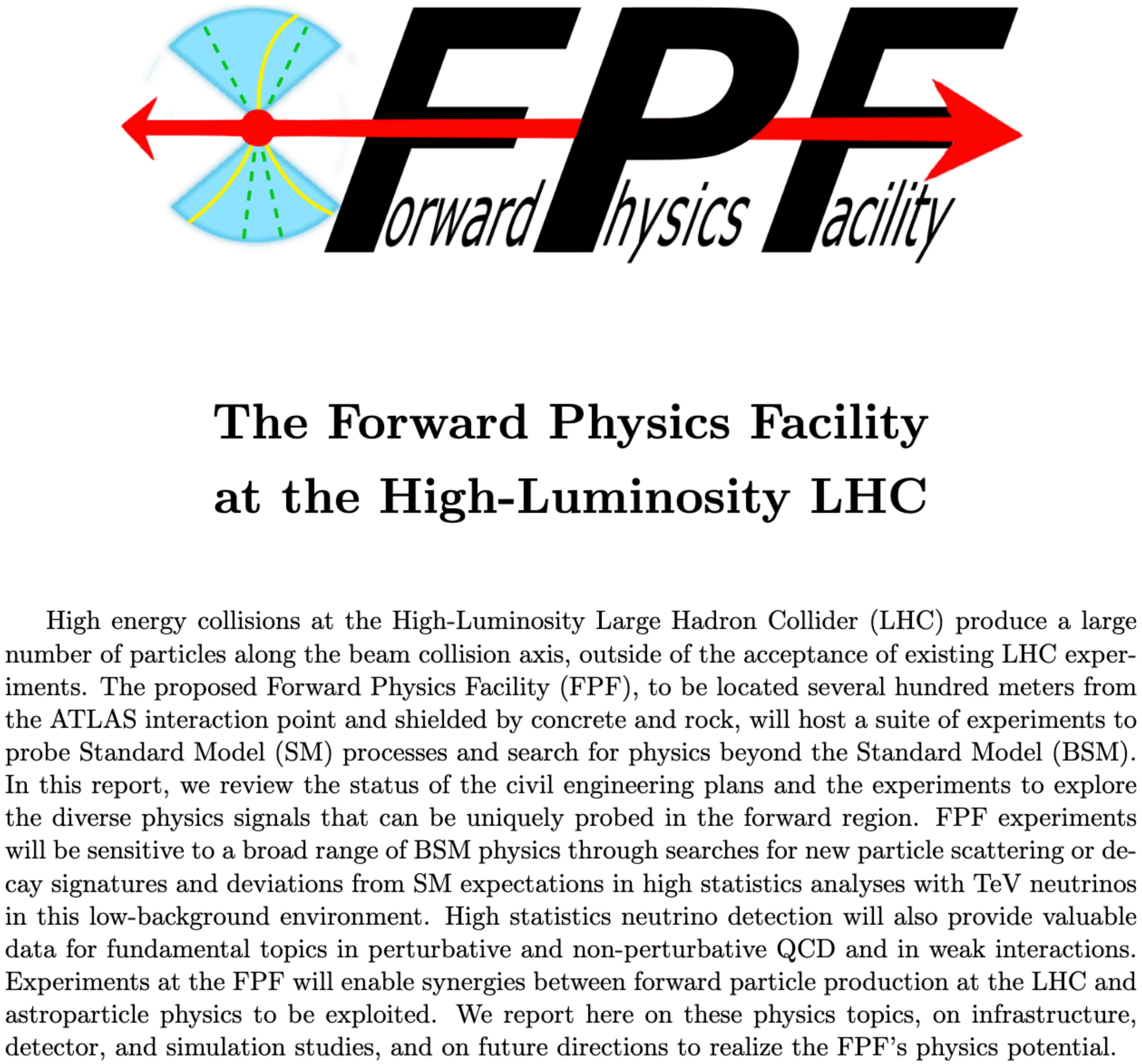

The Forward Physics Facility at the High-Luminosity LHC

High energy collisions at the High-Luminosity Large Hadron Collider (LHC) produce a large number of particles along the beam collision axis, outside of the acceptance of existing LHC experiments. The proposed Forward Physics Facility (FPF), to be located several hundred meters from the ATLAS interaction point and shielded by concrete and rock, will host a suite of experiments to probe Standard Model (SM) processes and search for physics beyond the Standard Model (BSM). In this report, we review the status of the civil engineering plans and the experiments to explore the diverse physics signals that can be uniquely probed in the forward region. FPF experiments will be sensitive to a broad range of BSM physics through searches for new particle scattering or decay signatures and deviations from SM expectations in high statistics analyses with TeV neutrinos in this low-background environment. High statistics neutrino detection will also provide valuable data for fundamental topics in perturbative and non-perturbative QCD and in weak interactions. Experiments at the FPF will enable synergies between forward particle production at the LHC and astroparticle physics to be exploited. We report here on these physics topics, on infrastructure, detector, and simulation studies, and on future directions to realize the FPF's physics potential.

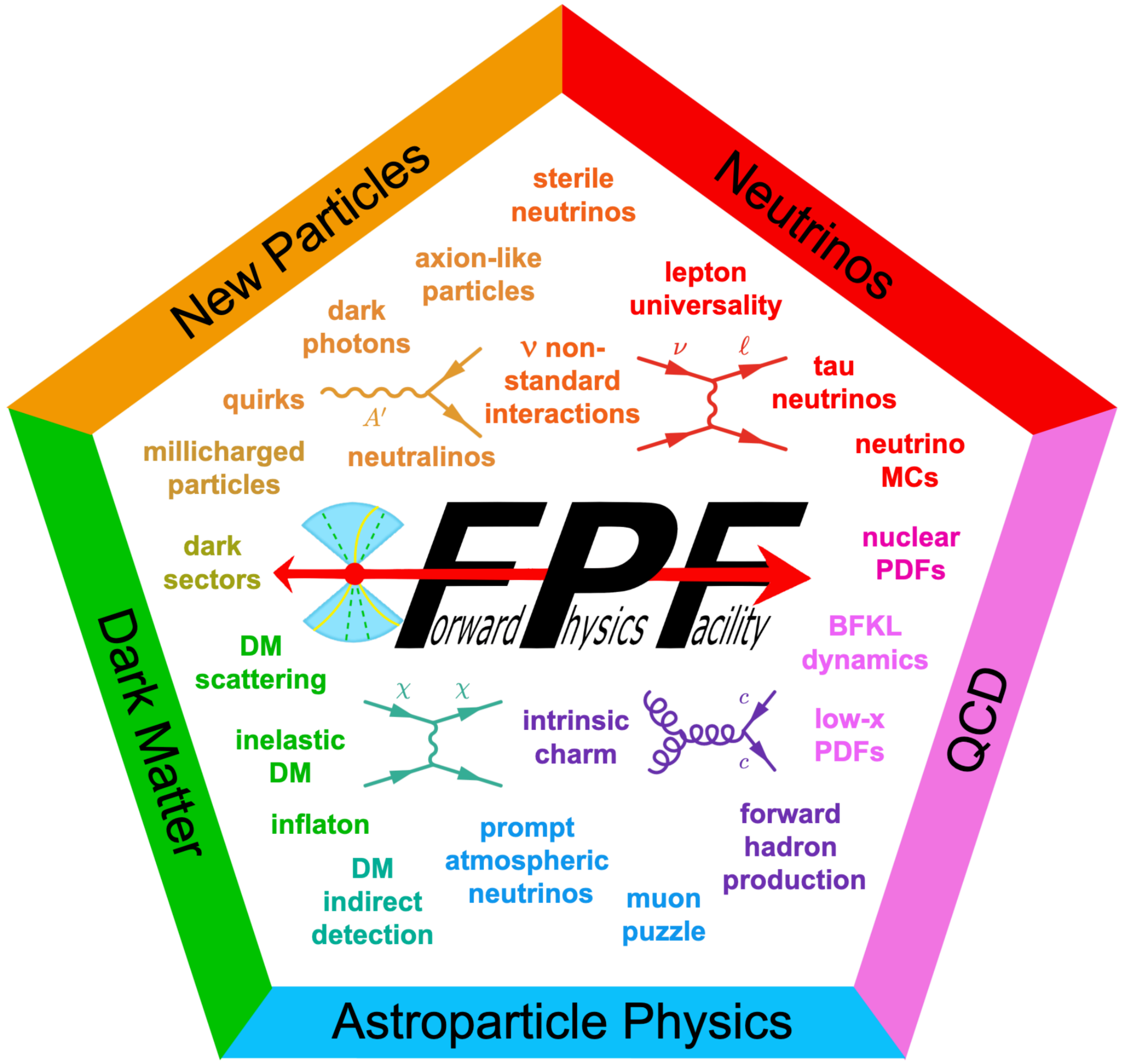

- **Fast progress from inception to installation**
- **Plan to start Civil Engineering during LS3**
- **Impressive advancements in studying physics' impacts (simulations, etc.)**

Physics Potential at Forward Physics Facility

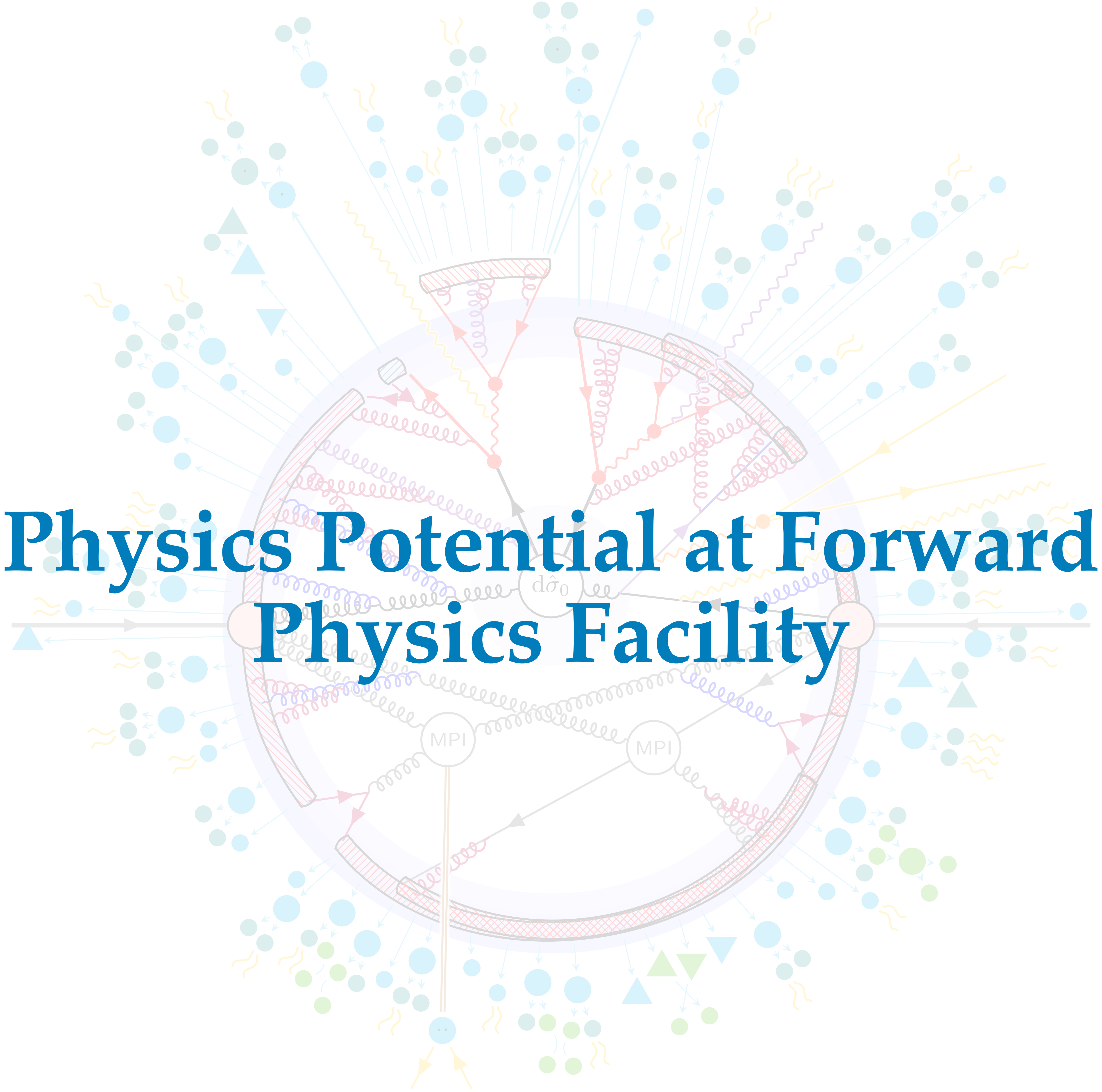

Neutrino Physics

- Forward neutrino detectors will measure neutrino cross sections at **unexplored TeV energies** for both NC and CC
- Unprecedented opportunities to study **Cosmic-Ray modelling** and **Muon puzzle**
- Further study **τ-neutrino** (through new light weekly coupled gauge boson decays) and **flavour universality**
- Improve and fine-tune neutrino **Monte Carlo (MC) Generators**

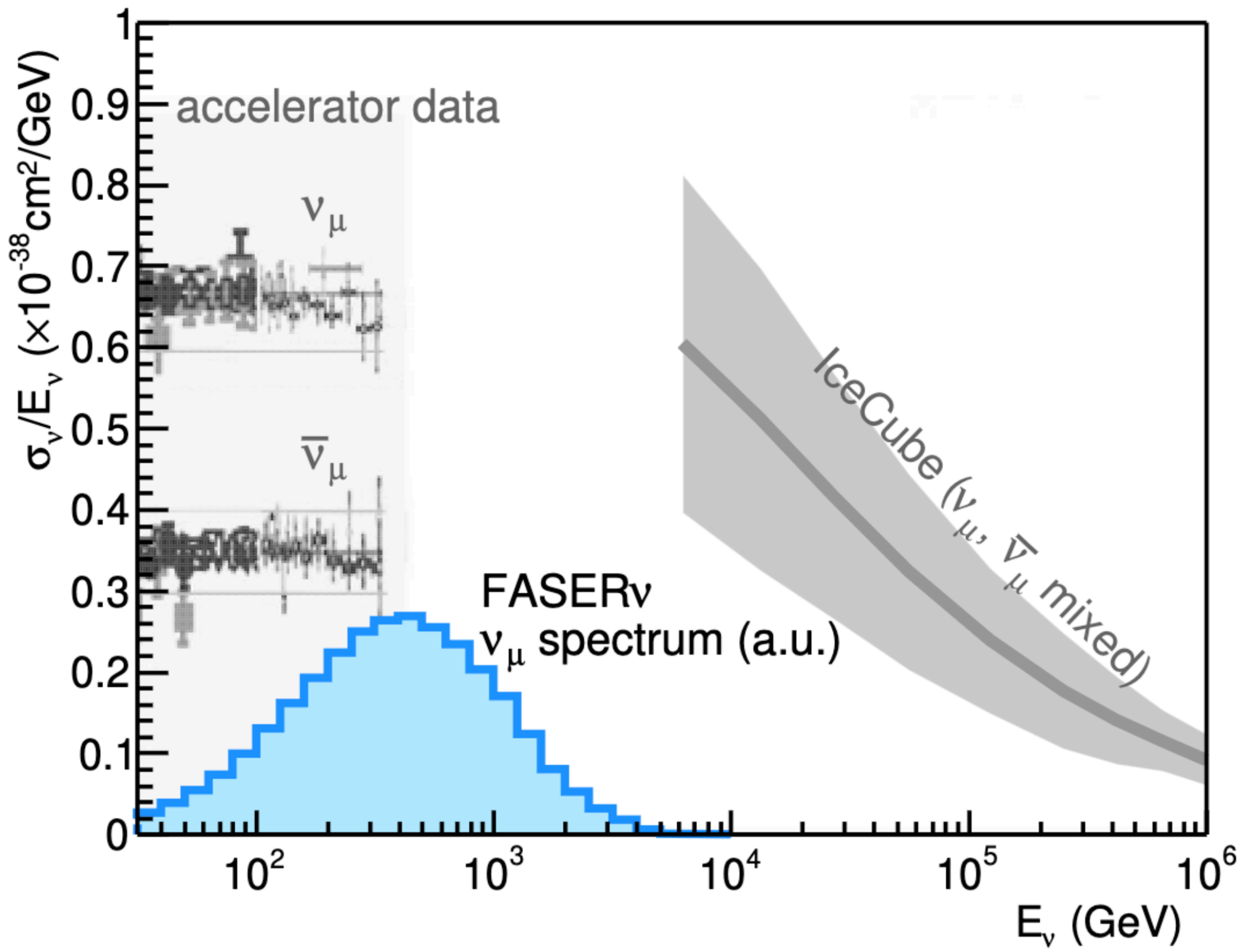

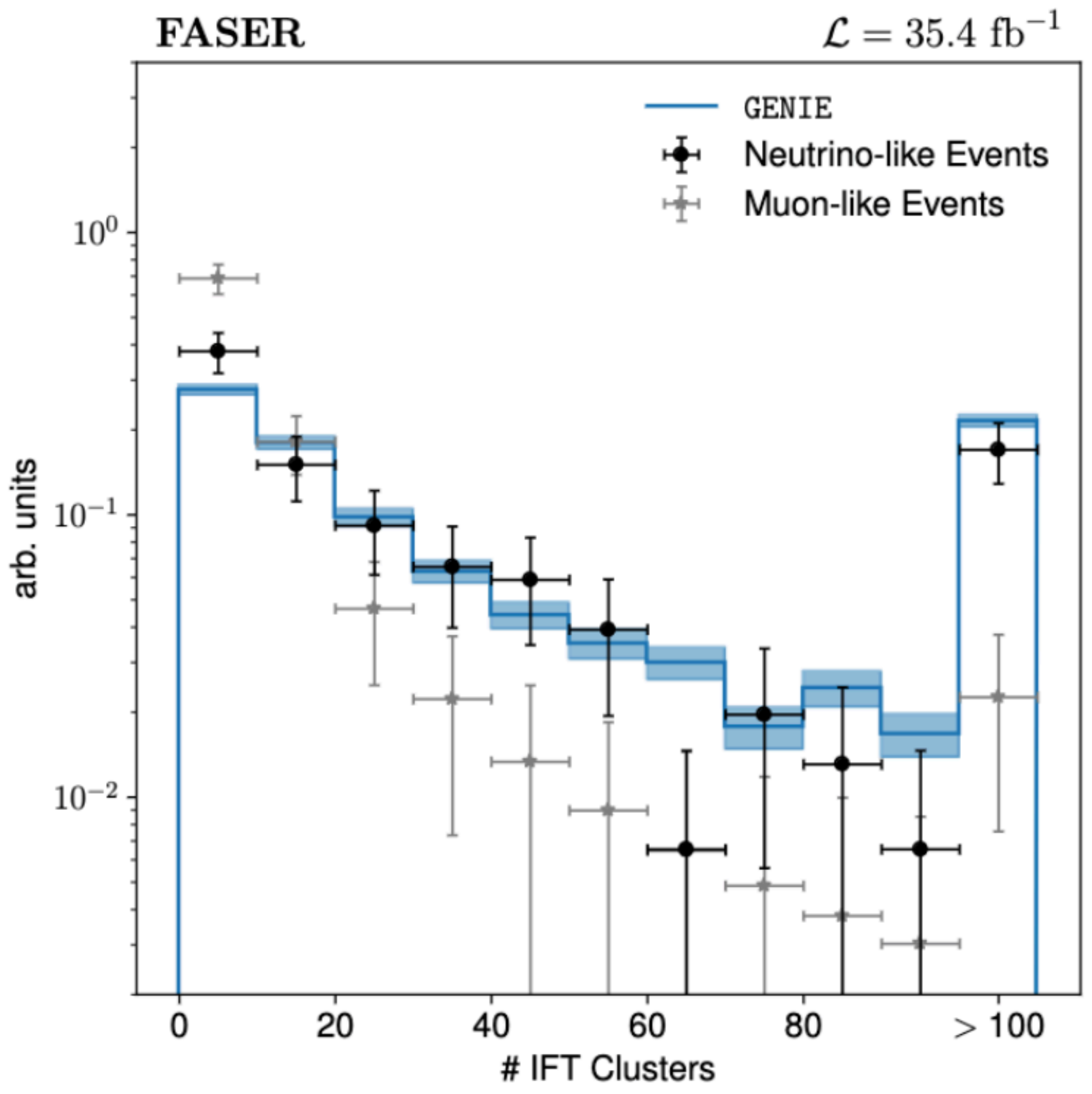

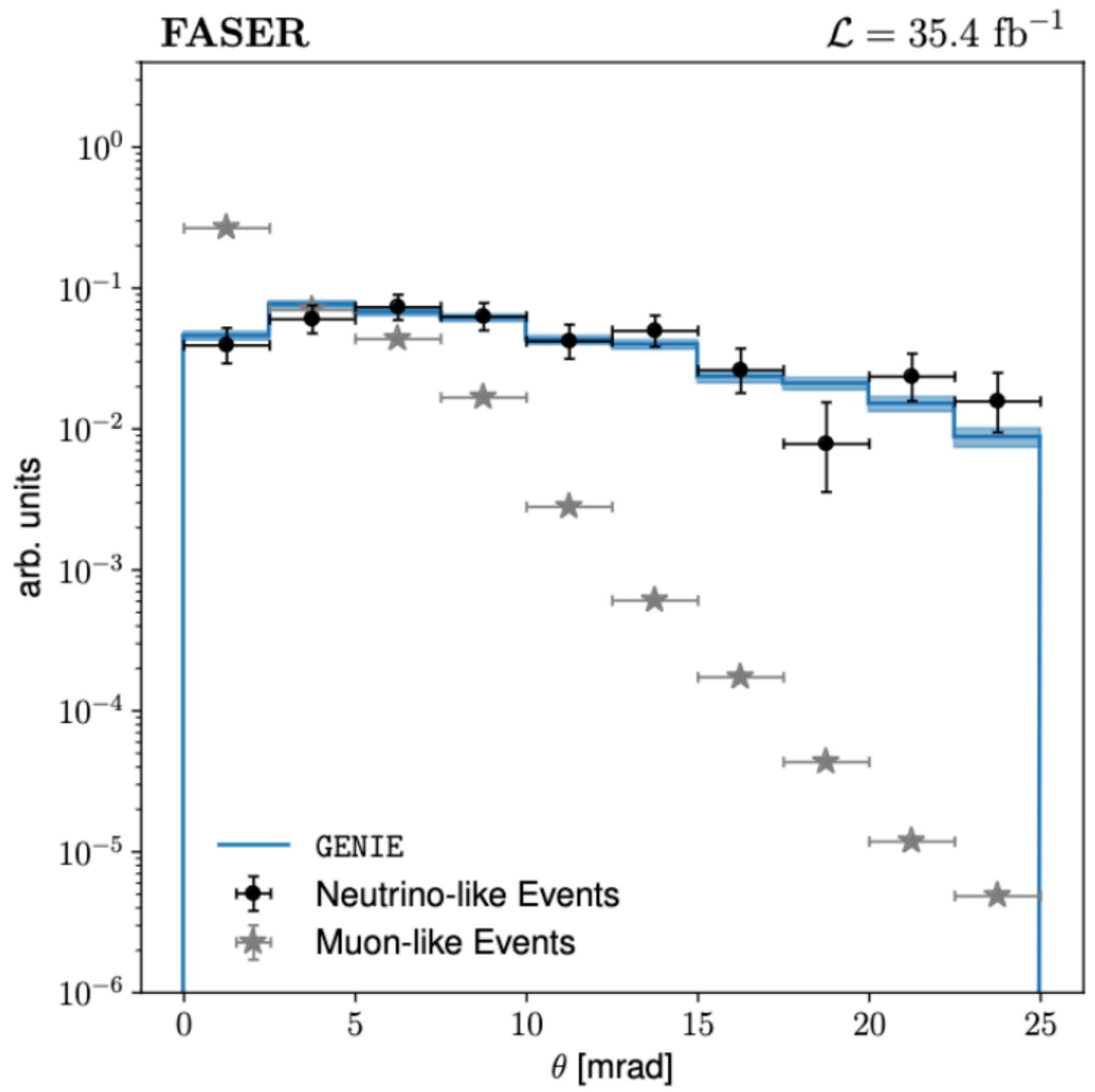

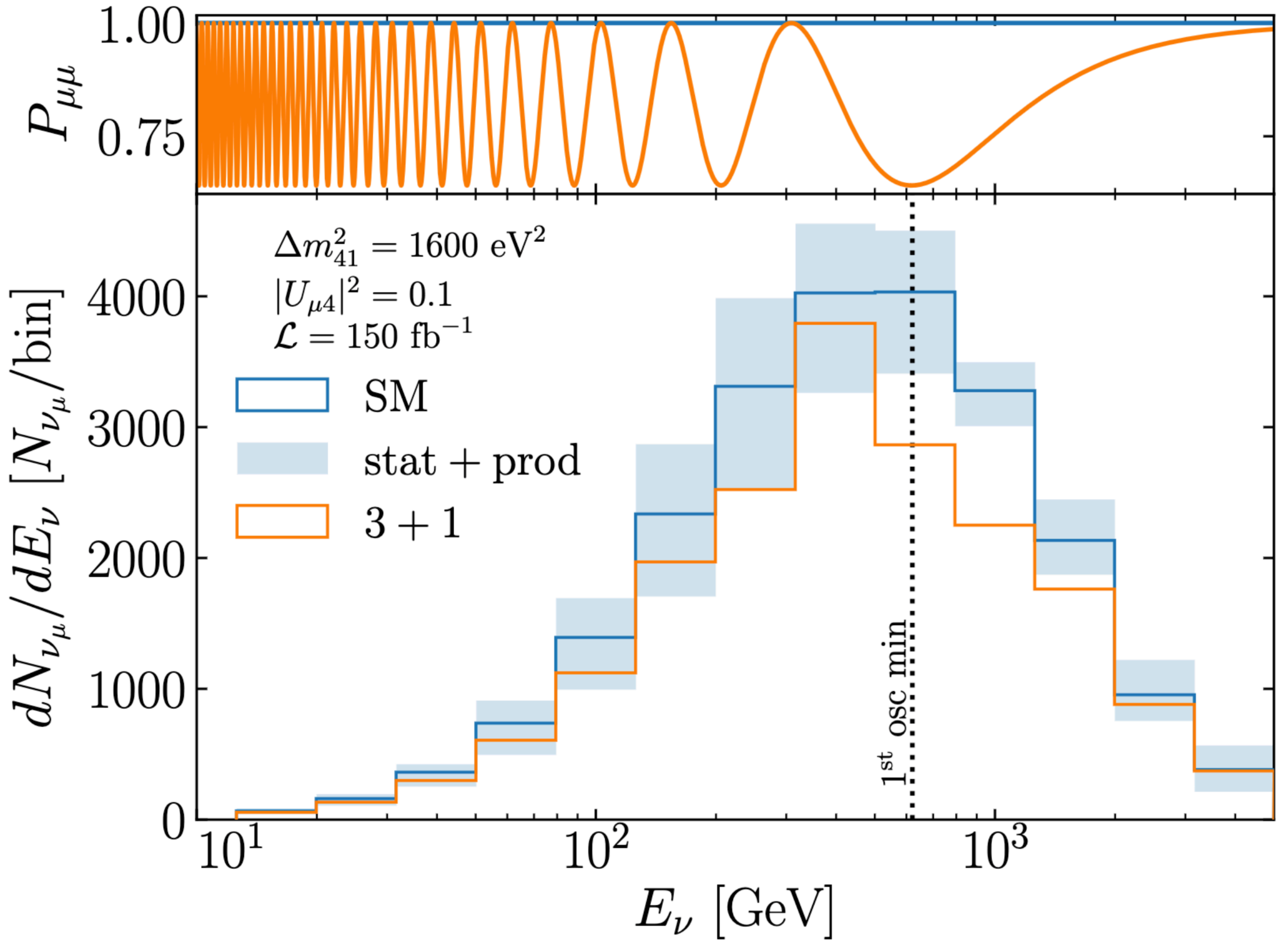

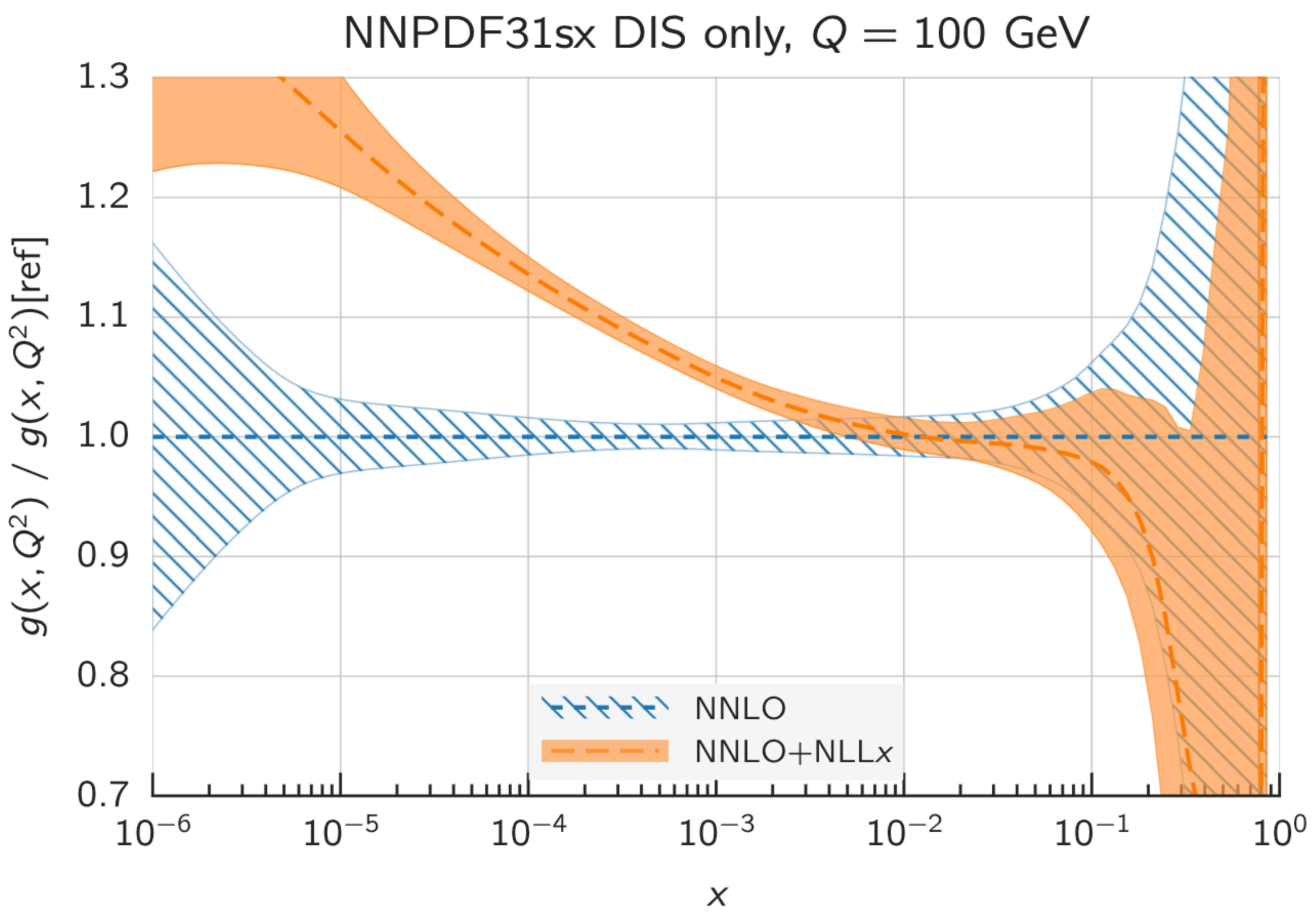

Hadron Substructure & QCD

- Explore **kinematic regions unavailable** to current and planned experiments
- Constrain PDFs via both NC and CC DIS neutrino scattering
- Improve determination of **D-meson Fragmentation**

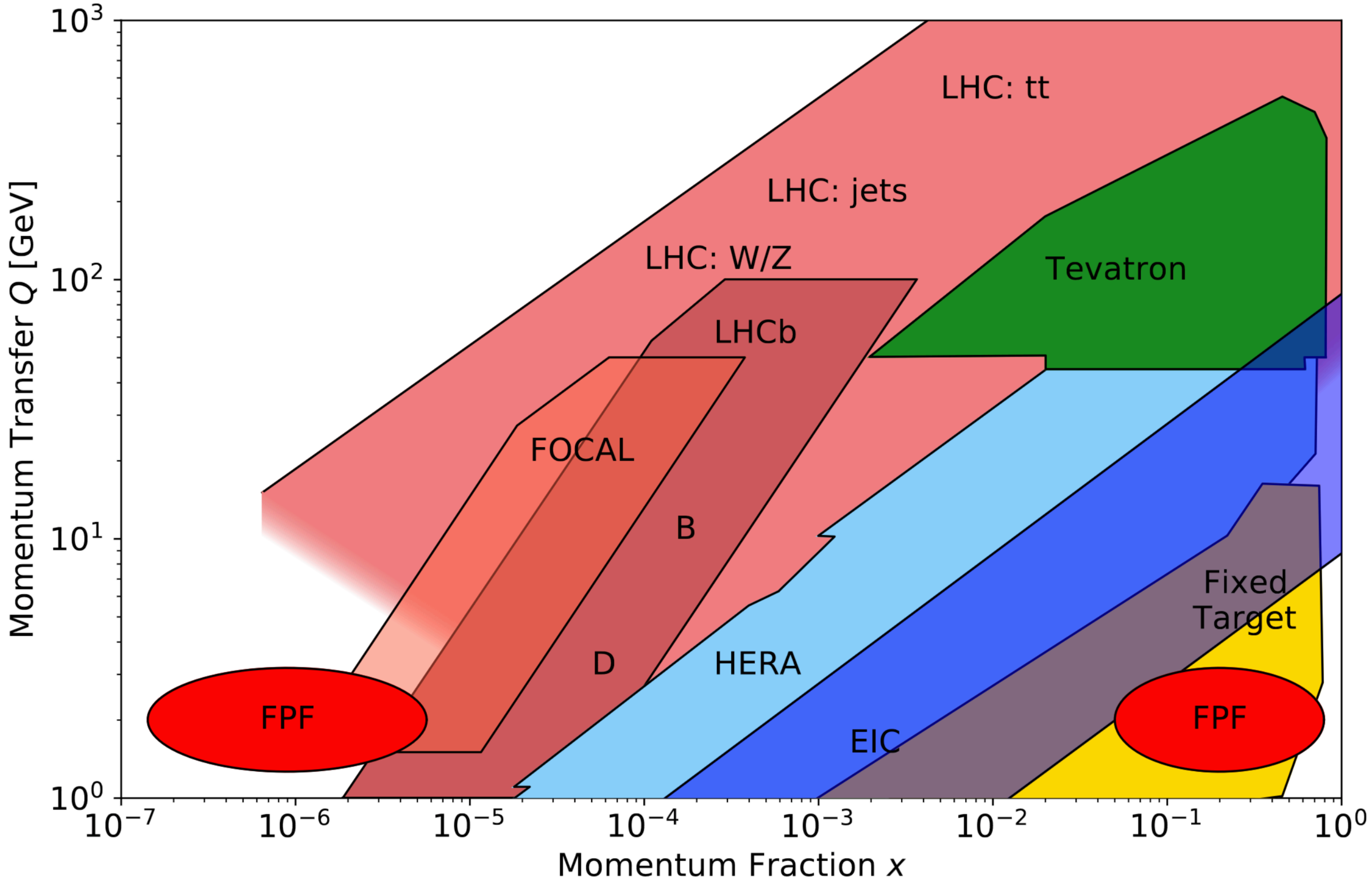

- Constrain **low-x gluon PDF** and **large-x (intrinsic charm)**
- Neutrino from Charm decay provide test-transition to **small-x factorisation** and **Gluon saturation**
- Improve predictions for cross-sections for Ultra-High Energy (UHE) astroparticle physics

Beyond Standard Model (BSM) Physics

Rich and Vast Beyond the Standard Model (BSM) scenarios can be studied at the FPF.

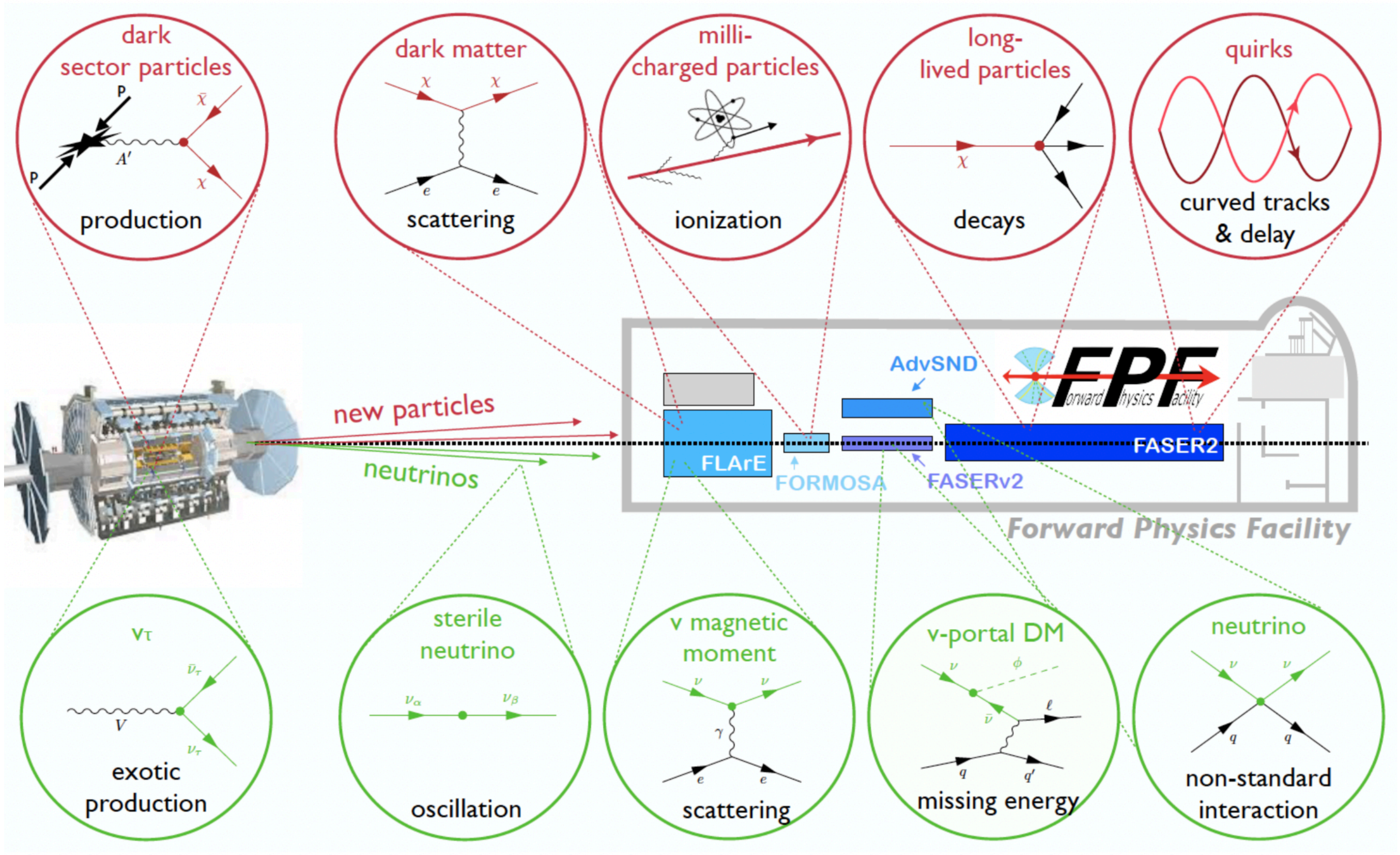

Hadron Structure with Neutrino DIS at the LHC

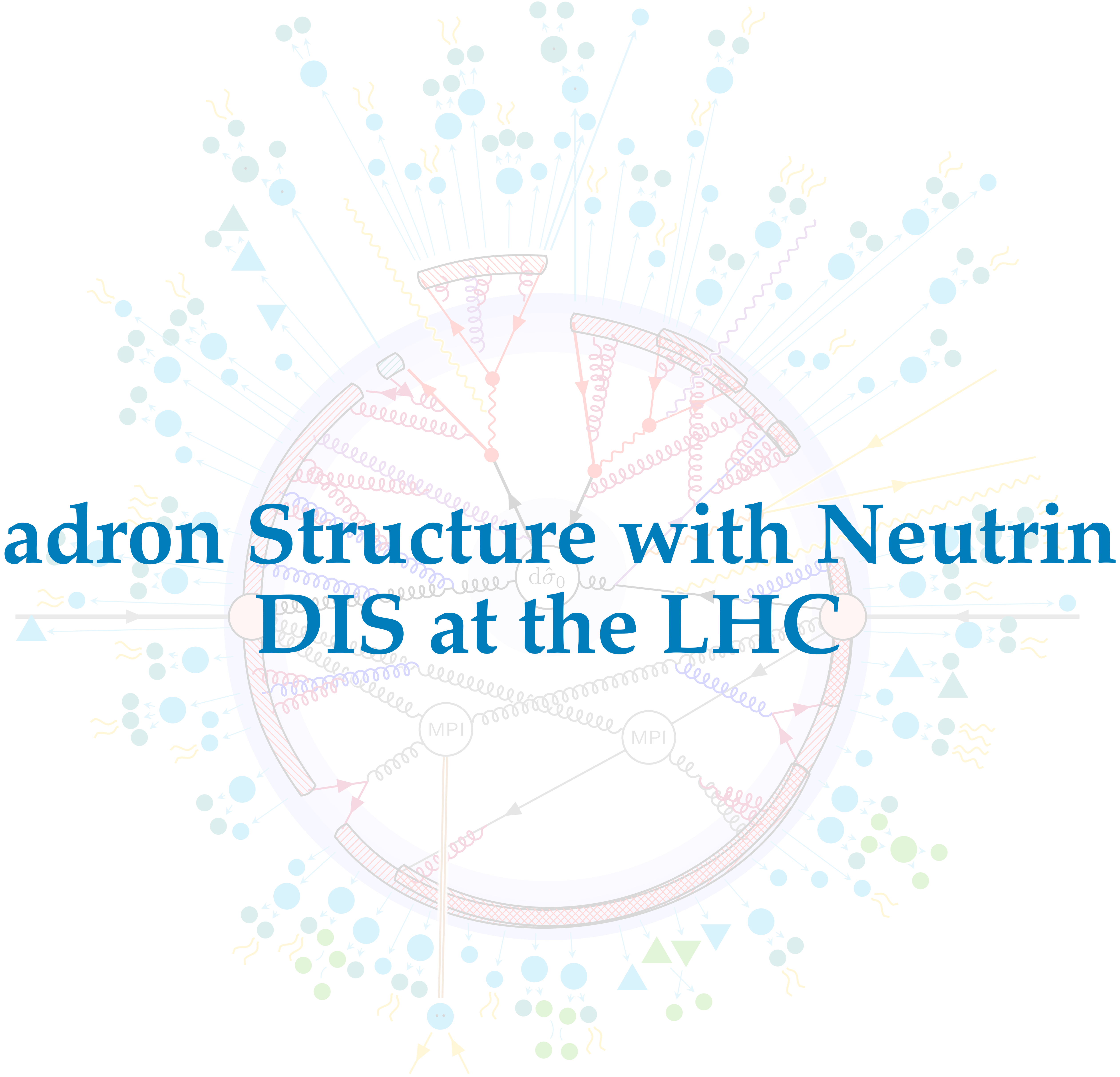

In Collaboration with M. Fieg, P. Krack, T. Mäkelä, J.C. Martinez, J. Rojo

SM Physics with LHC Neutrinos

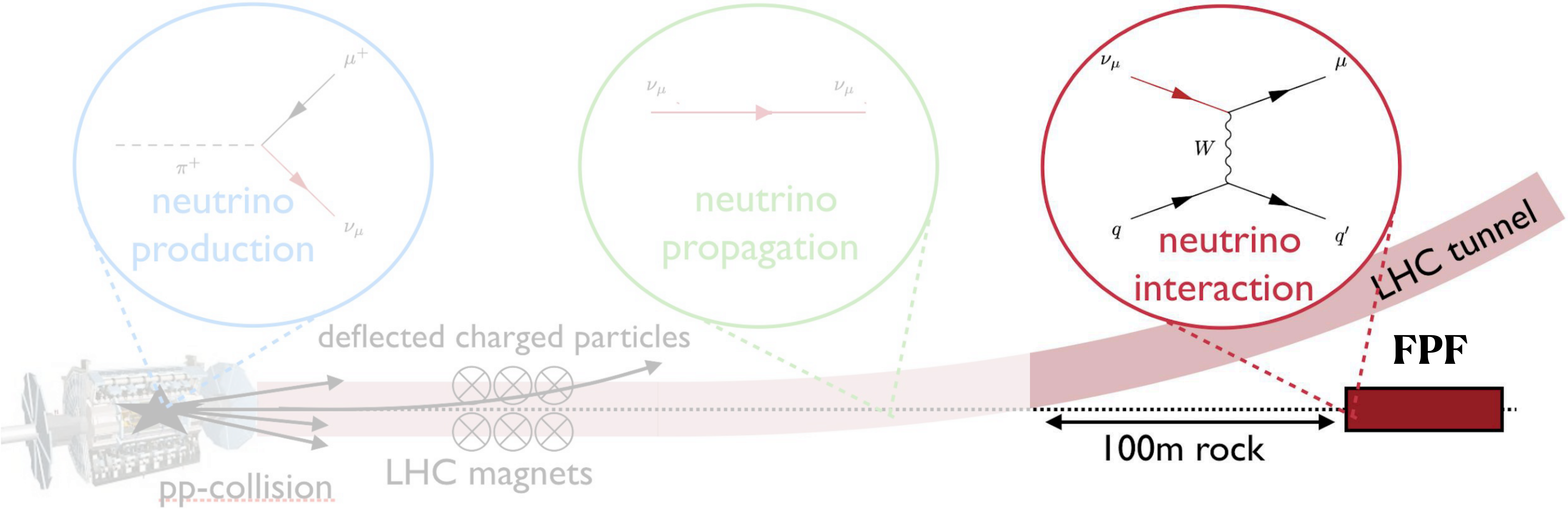

Neutrino-Nucleus interaction provide unprecedented opportunities.

- Sensitive information on nucleon and nuclear PDFs
- Quark & Anti-quark flavour separation including strangeness
- High Energy spectrum with very **large statistics (up to 1 million)**
- Complements current data by a factor of **10 both small-x and large-Q^2**

Lack of Dedicated Projections

Projection for Neutrino DIS @ LHC

- Provide state-of-the-art QCD calculations for **fully differential cross-sections**
- Consider both **inclusive** and **Charm production** (FASERν2)
- Generate DIS pseudo-data at current and proposed LHC experiments
- **Model systematic errors based on expected performance** for each LHC Run II and HL-LHC experiments

$$E_\nu = E_h + E_\ell$$

$$Q^2 = 4\left(E_h + E_\ell\right) E_\ell \sin^2\left(\theta_\ell/2\right)$$

$$x = \frac{4\left(E_h + E_\ell\right) E_\ell \sin^2\left(\theta_\ell/2\right)}{2 m_N E_h}$$

$$N^{(i)}_{\mathrm{ev,c}} = \boxed{n_T L_T} \boxed{\int_{Q^{2(i)}_{\mathrm{min}}}^{Q^{2(i)}_{\mathrm{max}}} \int_{x^{(i)}_{\mathrm{min}}}^{x^{(i)}_{\mathrm{max}}} \int_{E^{(i)}_{\mathrm{min}}}^{E^{(i)}_{\mathrm{max}}}} \boxed{\frac{dN_\nu\left(E_\nu\right)}{dE_\nu}} \boxed{\left(\frac{d^2\sigma^{\nu N \to \ell + c + X}\left(x, Q^2, E_\nu\right)}{dx\,dQ^2}\right)} \boxed{\mathscr{A}\left(x, Q^2, E_\nu\right)} dQ^2 dx dE_\nu$$

Detector Geometry

Kinematic Binning

Neutrino Fluxes

Differential Cross-Section

Acceptance

Experimental Acceptance & Performance

Detector	Rapidity	Target	Charge ID	Acceptance	Performance
FASERν	$\eta_\nu \geq 8.5$	Tungsten (1.1 tonnes)	muons	$E_\ell, E_h \gtrsim 100$ GeV $\tan\theta_\ell \lesssim 0.025$ reco E_h & charm ID	$\delta E_\ell \sim 30\%$ $\delta\theta_\ell \sim 0.06$ mrad $\delta E_h \sim 30\%$
SND@LHC	$7.2 \leq \eta_\nu \leq 8.4$	Tungsten (0.83 tonnes)	n/a	$E_\ell, E_h \gtrsim 20$ GeV $\theta_\mu \lesssim 0.15, \theta_e \lesssim 0.5$	n/a
FASERν2	$\eta_\nu \geq 8.5$	Tungsten (20 tonnes)	muons	$E_\ell, E_h \gtrsim 100$ GeV $\tan\theta_\ell \lesssim 0.05$ reco E_h & charm ID	$\delta E_\ell \sim 30\%$ $\delta\theta_\ell \sim 0.06$ mrad $\delta E_h \sim 30\%$
AdvSND-far	$7.2 \leq \eta_\nu \leq 8.4$	Tungsten (5 tonnes)	muons	$E_\ell, E_h \gtrsim 20$ GeV $\theta_\mu \lesssim 0.15, \theta_e \lesssim 0.5$ reco E_h	n/a
FLArE (*)	$\eta_\nu \geq 7.5$	LAr (10, 100 tonnes)	muons	$E_\ell, E_h \gtrsim 2$ GeV, $E_e \lesssim 2$ TeV $\theta_\mu \lesssim 0.025$, $\theta_e \lesssim 0.5$ reco E_h	$\delta E_e \sim 5\%$, $\delta E_\mu \sim 30\%$ $\delta\theta_\ell \sim 15$ mrad $\delta E_h \sim 30\%$

LHC Run III
$\mathscr{L} = 150$ fb^{-1}

Current estimate of the experimental acceptance and performance; may subject to change in final realisation.

LHC Run III
$\mathscr{L} = 3$ ab^{-1}

FPF Pseudodata Generation: Integrated Event Rate

Detector	N_{ν_e}	$N_{\bar{\nu}_e}$	$N_{\nu_e} + N_{\bar{\nu}_e}$	N_{ν_μ}	$N_{\bar{\nu}_\mu}$	$N_{\nu_\mu} + N_{\bar{\nu}_\mu}$
FASERν	0.2k (31)	110 (19)	0.3k (50)	0.6k (98)	0.3k (45)	0.9k (140)
SND@LHC	88 (11)	38 (5.4)	130 (16)	0.3k (54)	96 (22)	0.4k (76)
FASERν2	58k (8.3k)	28k (5.0k)	86k (13.3k)	190k (27k)	67k (12k)	260k (39k)
AdvSND-far	5.9k (0.7k)	2.8k (0.4k)	8.7k (1.1k)	20k (2.4k)	8k (1.1k)	28k (3.5k)
FLArE10	22k (2.7k)	10k (1.5k)	32k (4.2k)	38k (5.2k)	19k (2.5k)	57k (7.7k)
FLArE100	140k (18k)	66k (9.5k)	210k (27k)	220k (30k)	120k (15k)	340k (45k)

Integrated Event Rates for Inclusive (Charm) production for DIS Kins.

- μ-neutrino yields largest Event Rates and Smaller Production Uncertainties
- FASERν2 and FLArE100 is expected to record highest event rates
- Ideal-case scenario is combined measurements $\Longleftrightarrow$ systematics cross-calibration

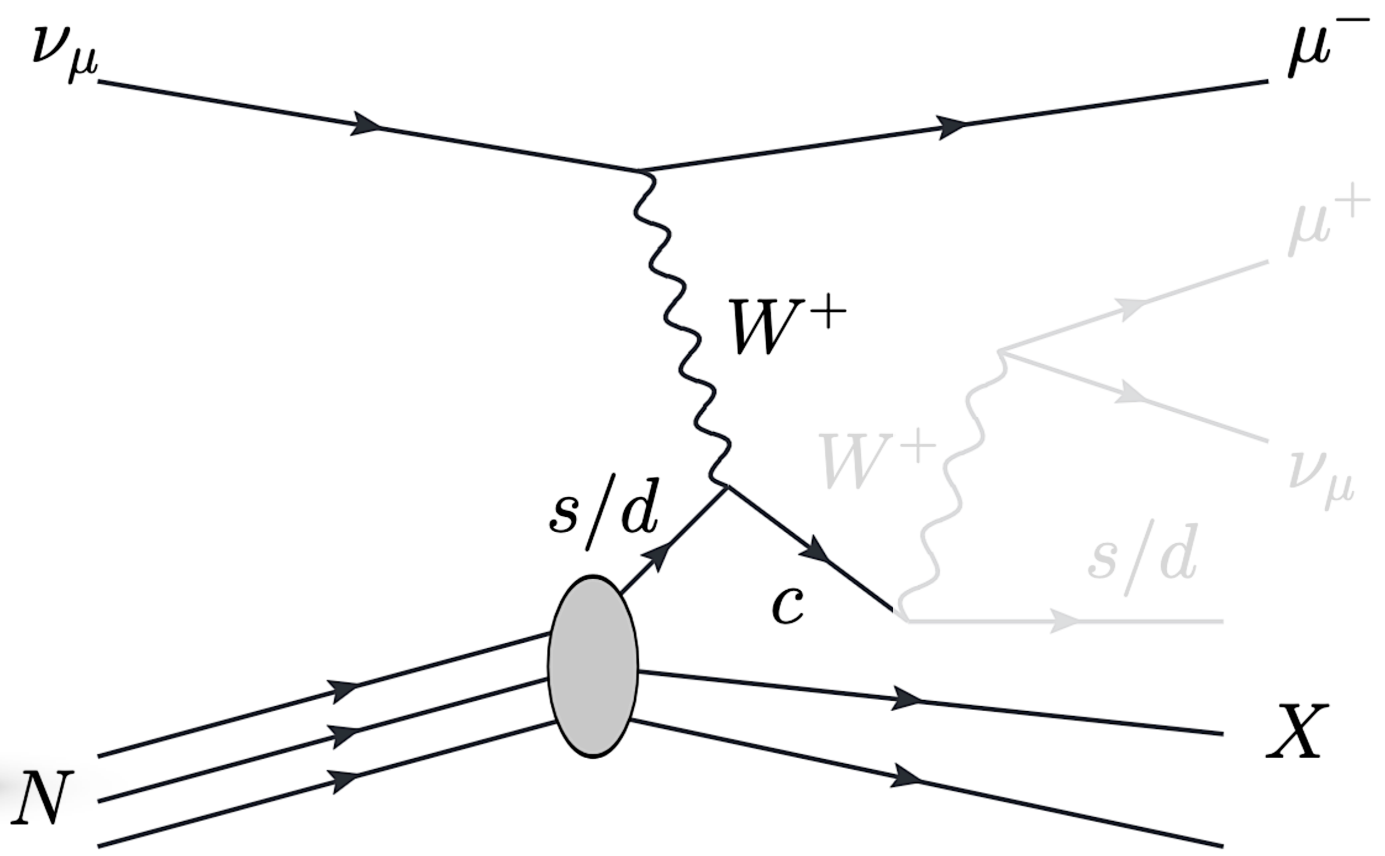

FPF Pseudodata Generation: Kinematic Coverage & Nb Events

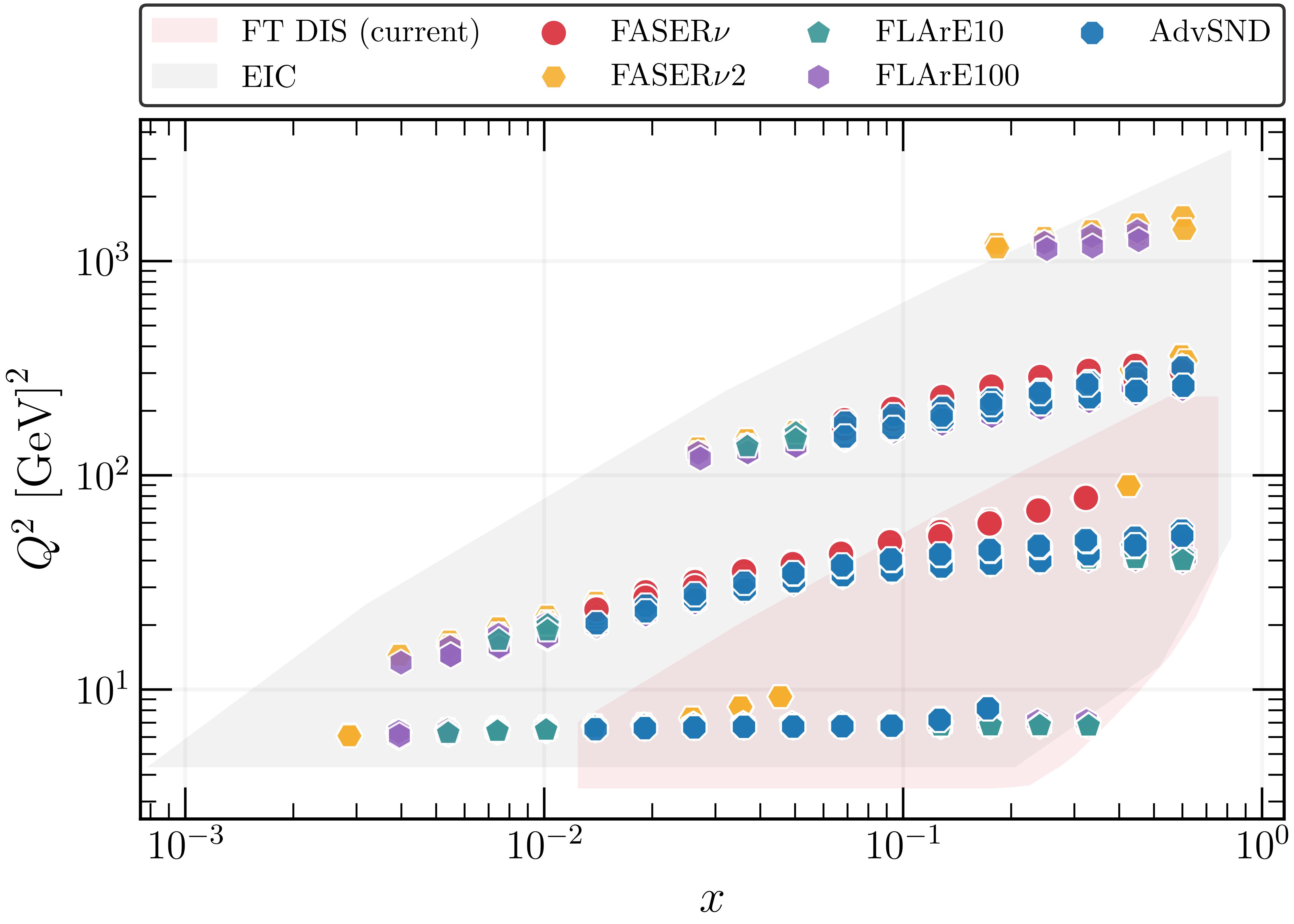

Number of DIS Events per Bin

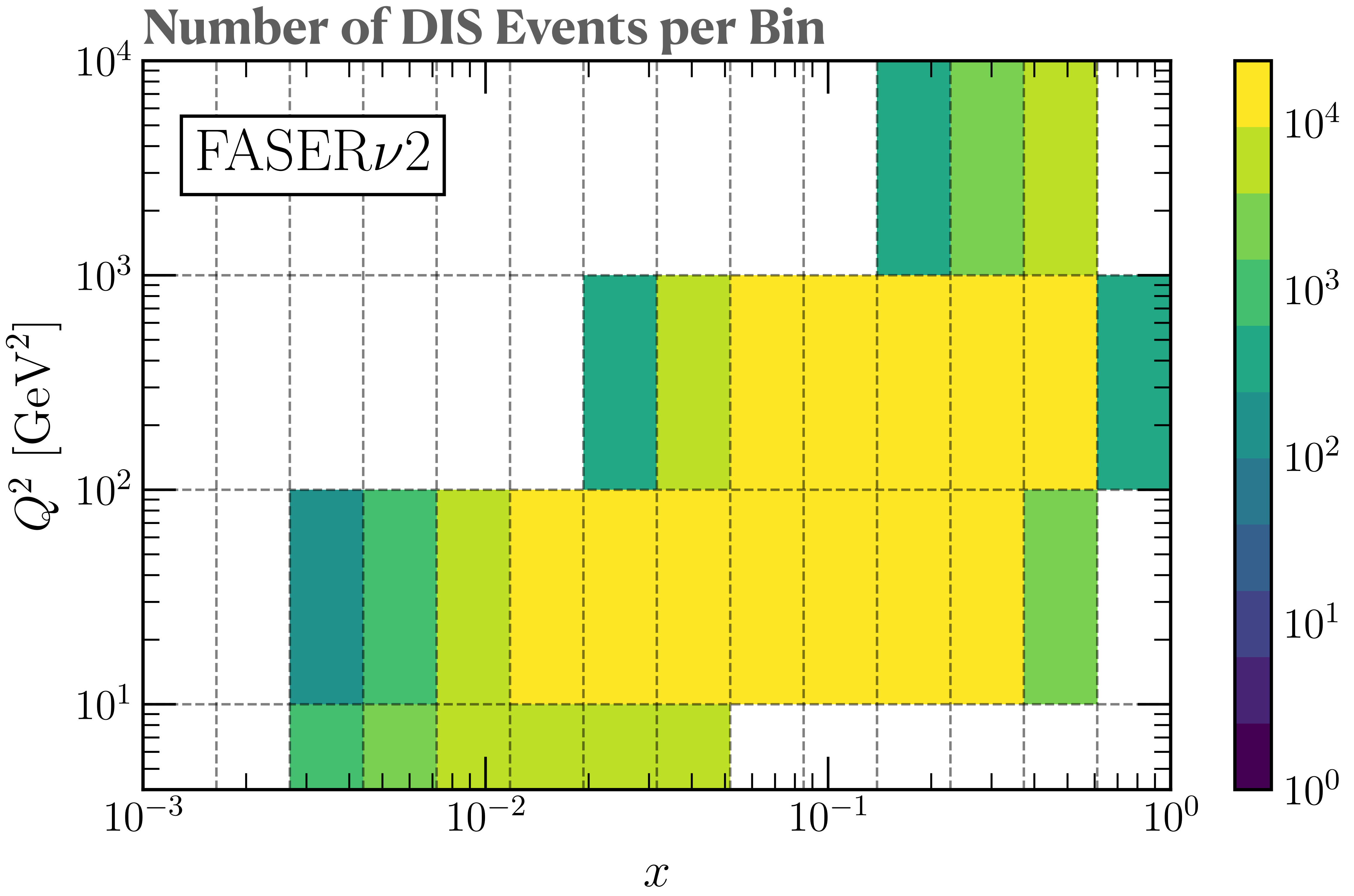

- Expand kinematic coverage of existing (Neutrino-Nucleus) experiments by an **order of magnitude in x and Q^2**
- Charged-current counterpart of EIC (Electron Ion Collider) in a comparable region of Phase Space
- Large event rates for most kinematic region covered $\Longrightarrow$ **Statistical Uncertainties $\mathcal{O}(1\%)$ or Smaller**

FPF Pseudodata Generation: Projected Uncertainties

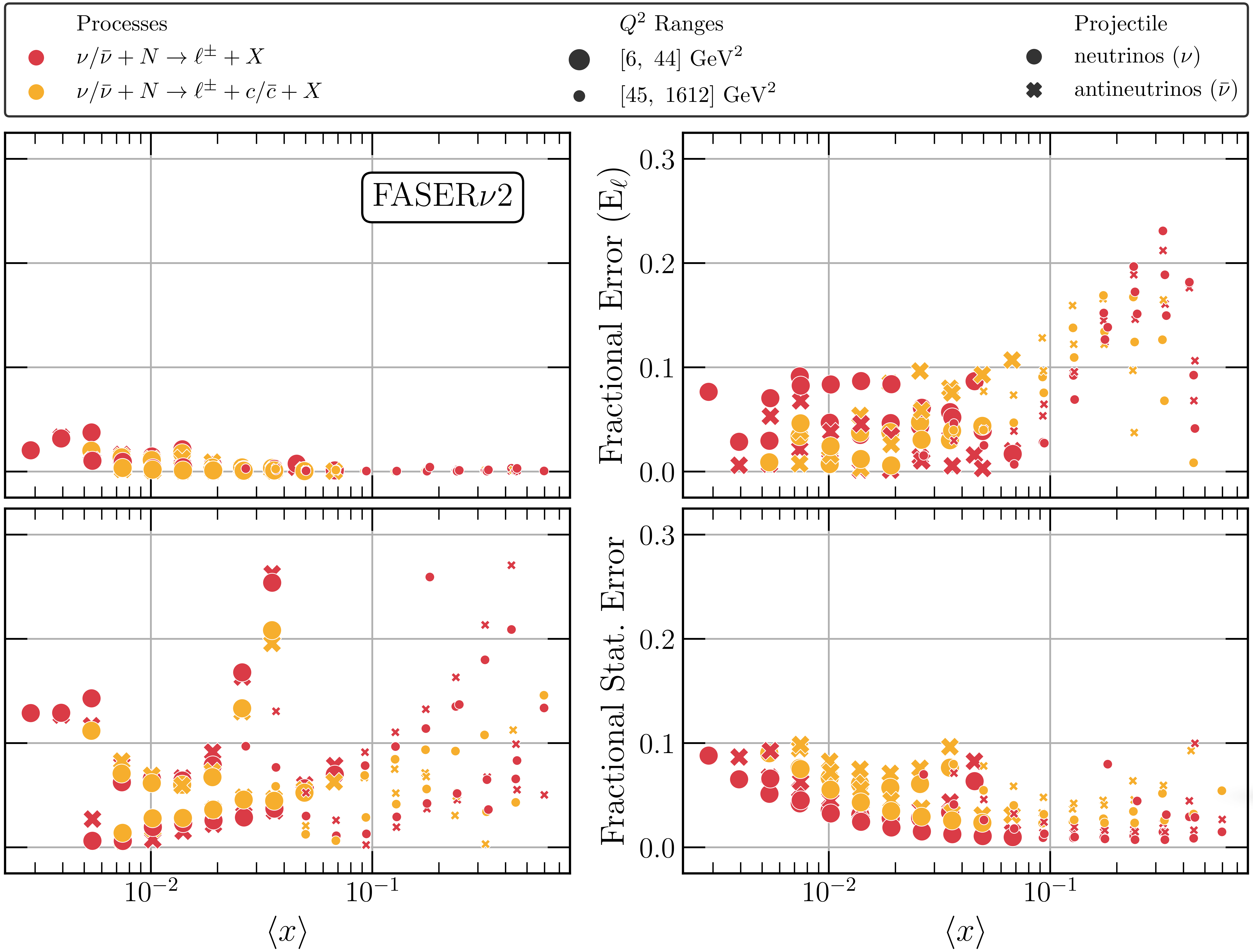

- Systematic uncertainties associated to final-state energy E_h **and E_ℓ range from** $1\,\%$ **to** $\mathcal{O}(1)$
- Systematic uncertainties associated to scattering angle θ are generally below $\mathcal{O}(1\%)$
- **Statistical uncertainties are subdominant** (below $\mathcal{O}(1\%)$) $\Longleftrightarrow$ Current **LHC experiments are limited by** Statistics while FPF might be limited by Systematics.

Impacts on Nuclear PDFs (Tungsten)

Using the profiling method applied to Hessian PDFs using the xFitter framework.

$$\chi^2 = \sum_{i=1}^{N_{\rm bin}} \frac{\left(\mathcal{O}_i^{(\rm exp)} + \Gamma_i^{\alpha,{\rm exp}} b_\alpha^{(\rm exp)} - \mathcal{O}_i^{(\rm th)} - \Gamma_i^{\beta,{\rm th}} b_\beta^{(\rm th)}\right)^2}{\left(\delta^{(\rm stat)}\mathcal{O}_i^{(\rm th)}\right)^2} + \sum_\alpha \left(b_\alpha^{(\rm exp)}\right)^2 + T^2 \sum_\beta \left(b_\beta^{(\rm th)}\right)^2$$

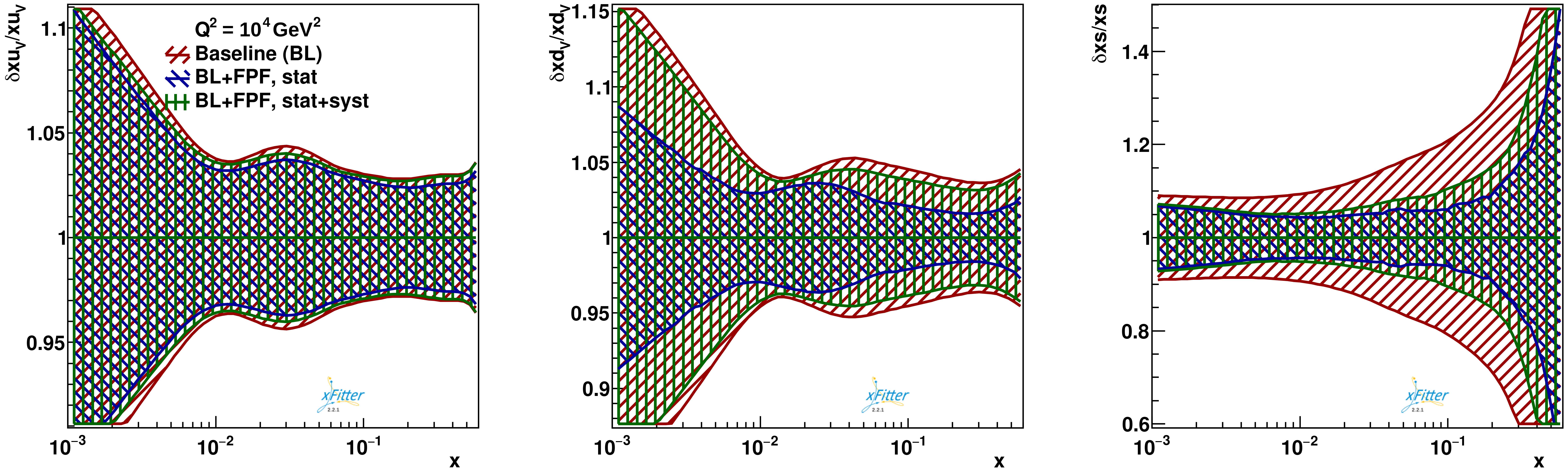

Impacts on Proton PDFs

Using the profiling method applied to Hessian PDFs using the xFitter framework.

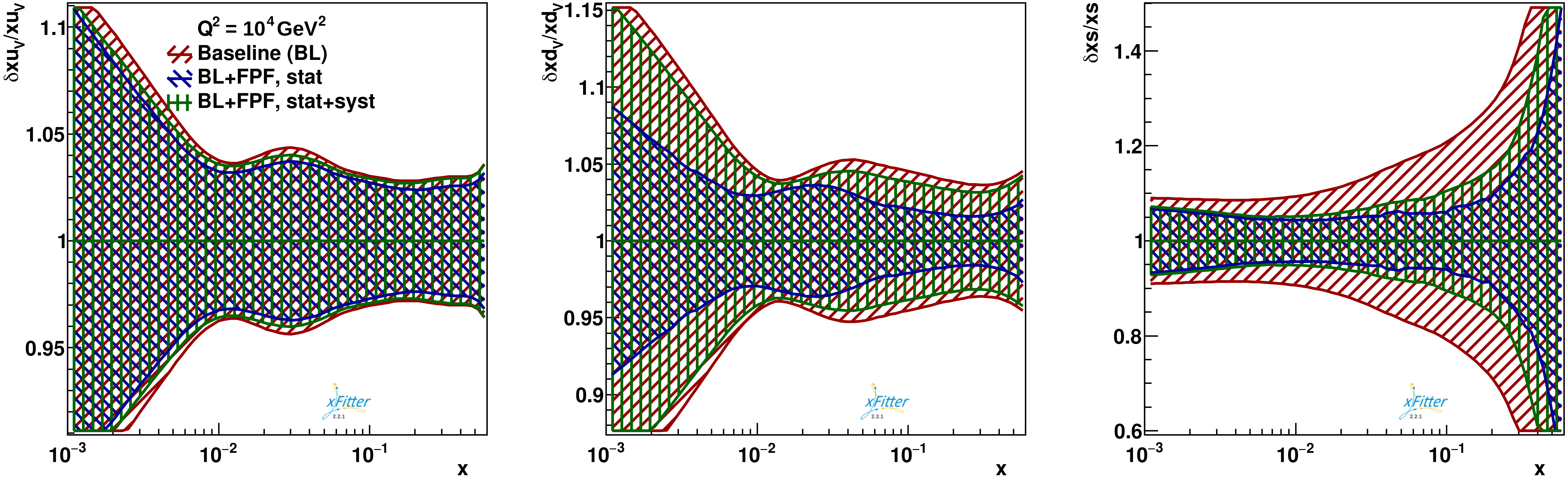

- Strong impacts on the up & down valence quarks and strangeness
- For a rather conservative estimate of the Systematic, Systematic Uncertainties present some limitations
- PDF determination improve with LHC neutrino enhance HL-LHC measurements (W mass, etc.)

Impact on Proton PDFs

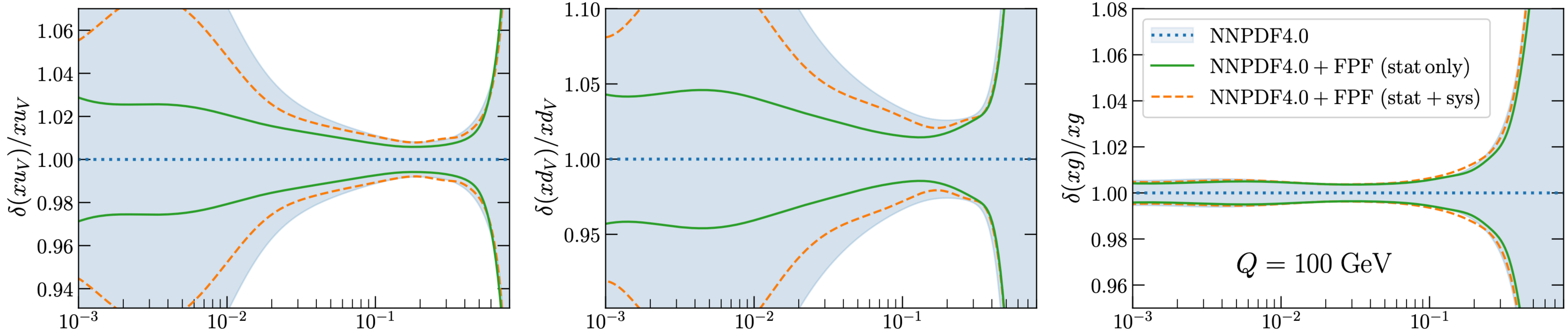

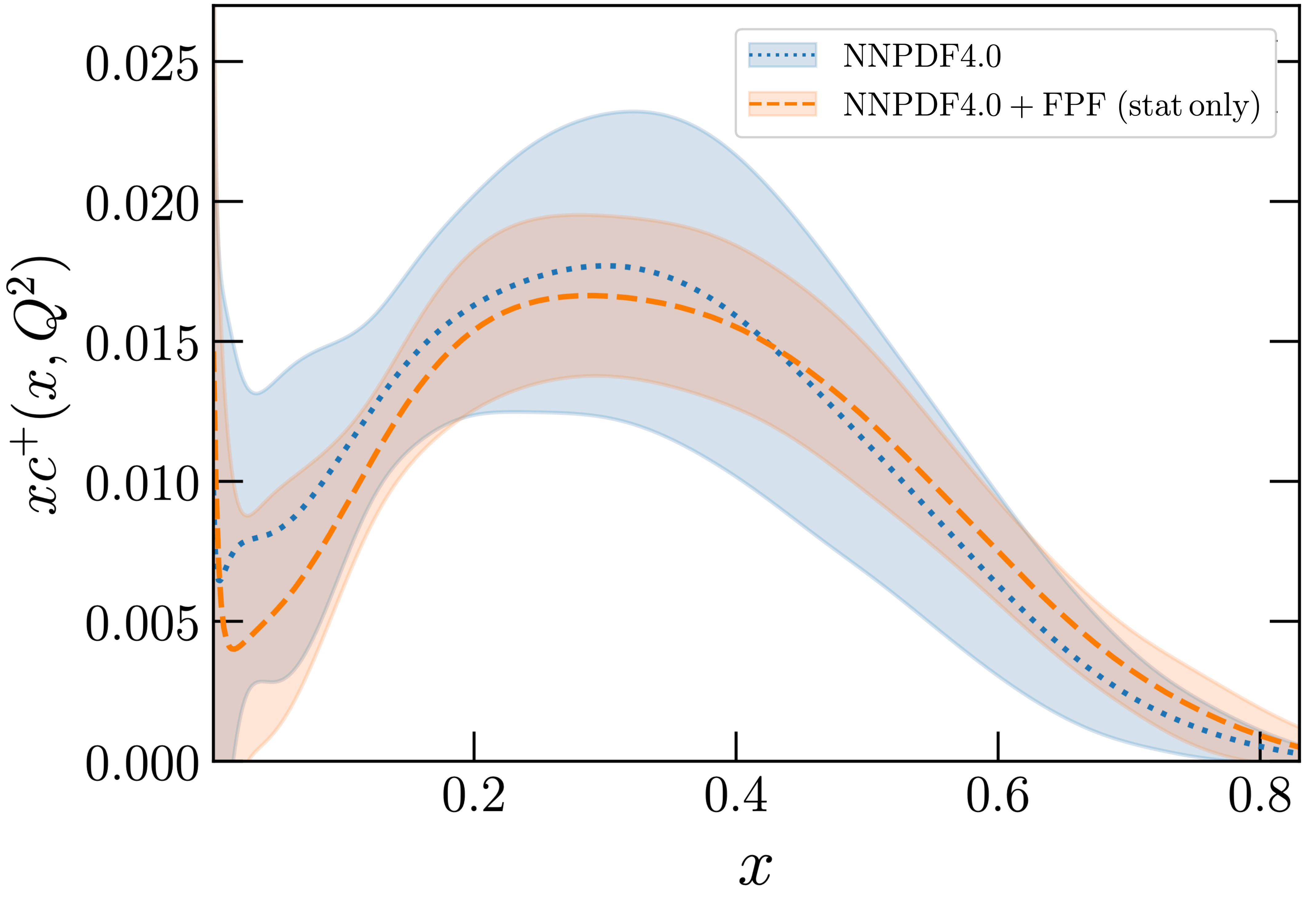

- Consistent with xFitter determination (very different methodologies)
- Negligible impact on the gluon distribution (even when only accounting for statistical errors)
- Provides more information on large-*x* charm PDF

Stability on Proton PDF Determination

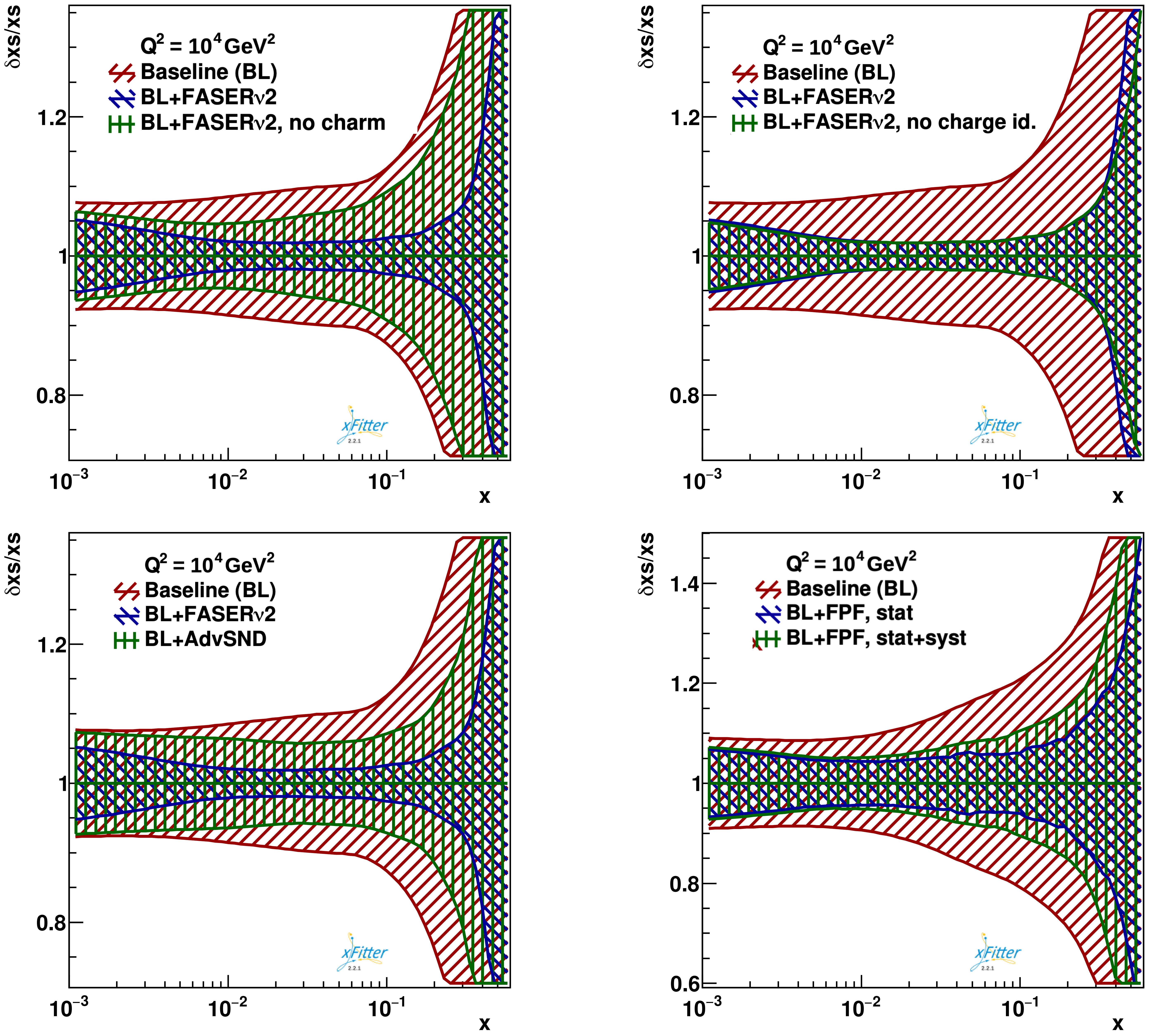

- **Charm-Tagged measurements** are **important** for precision the study of hadron structure
- Charged-lepton identification does not provide significant impacts
- PDF sensitivity largely dominated by **FASERν2** $\Longleftrightarrow$ Including all FPF experiments yields results closer to FASERν2

Impacts on (HL-)LHC Phenomenology

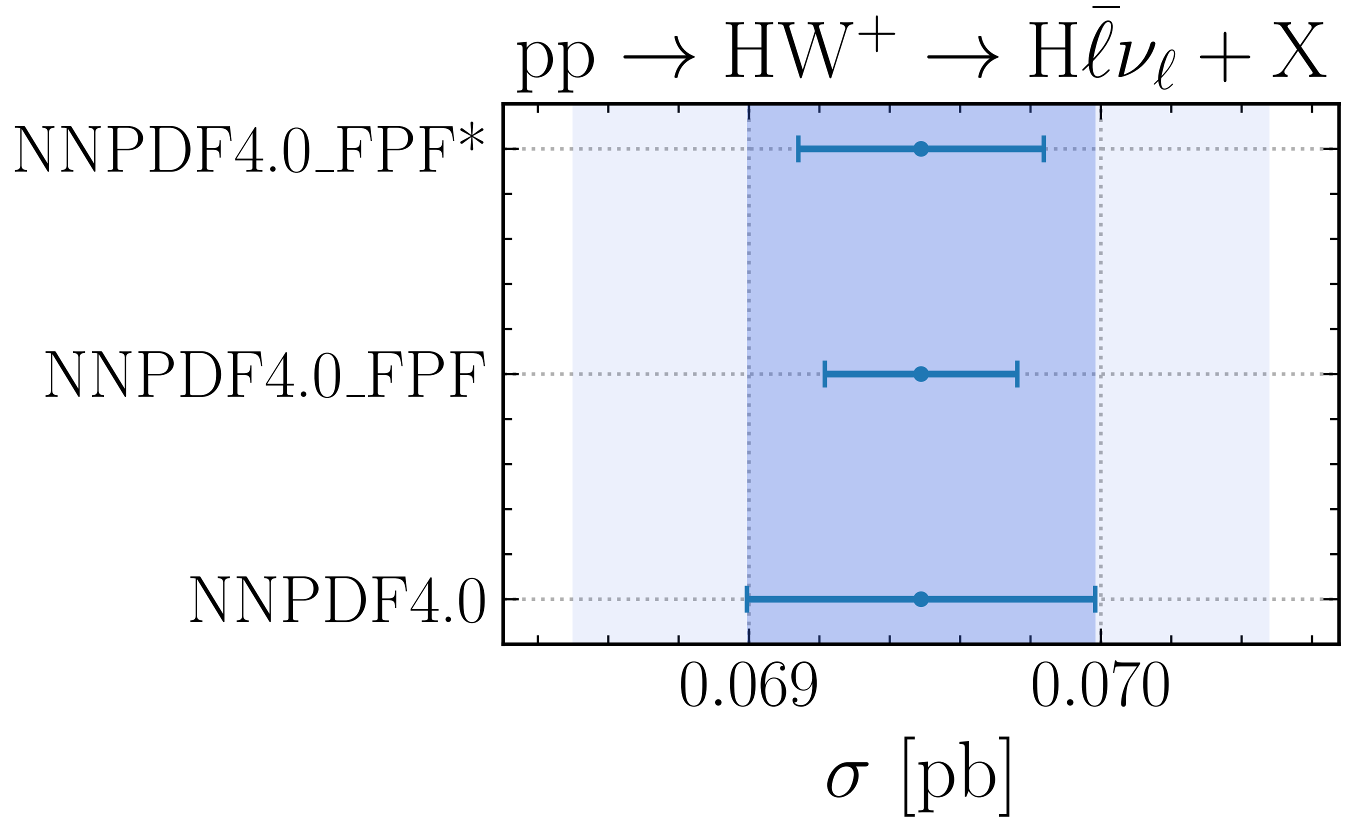

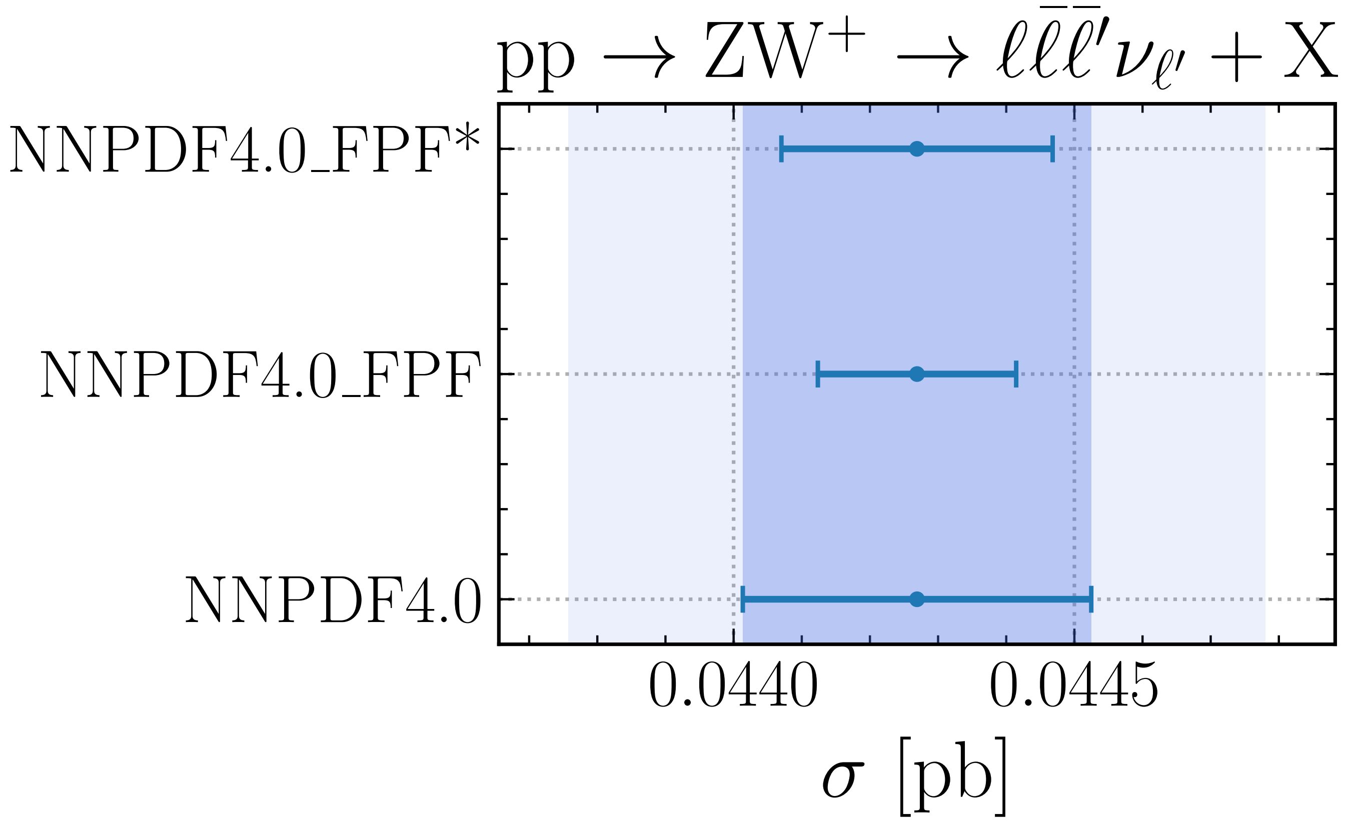

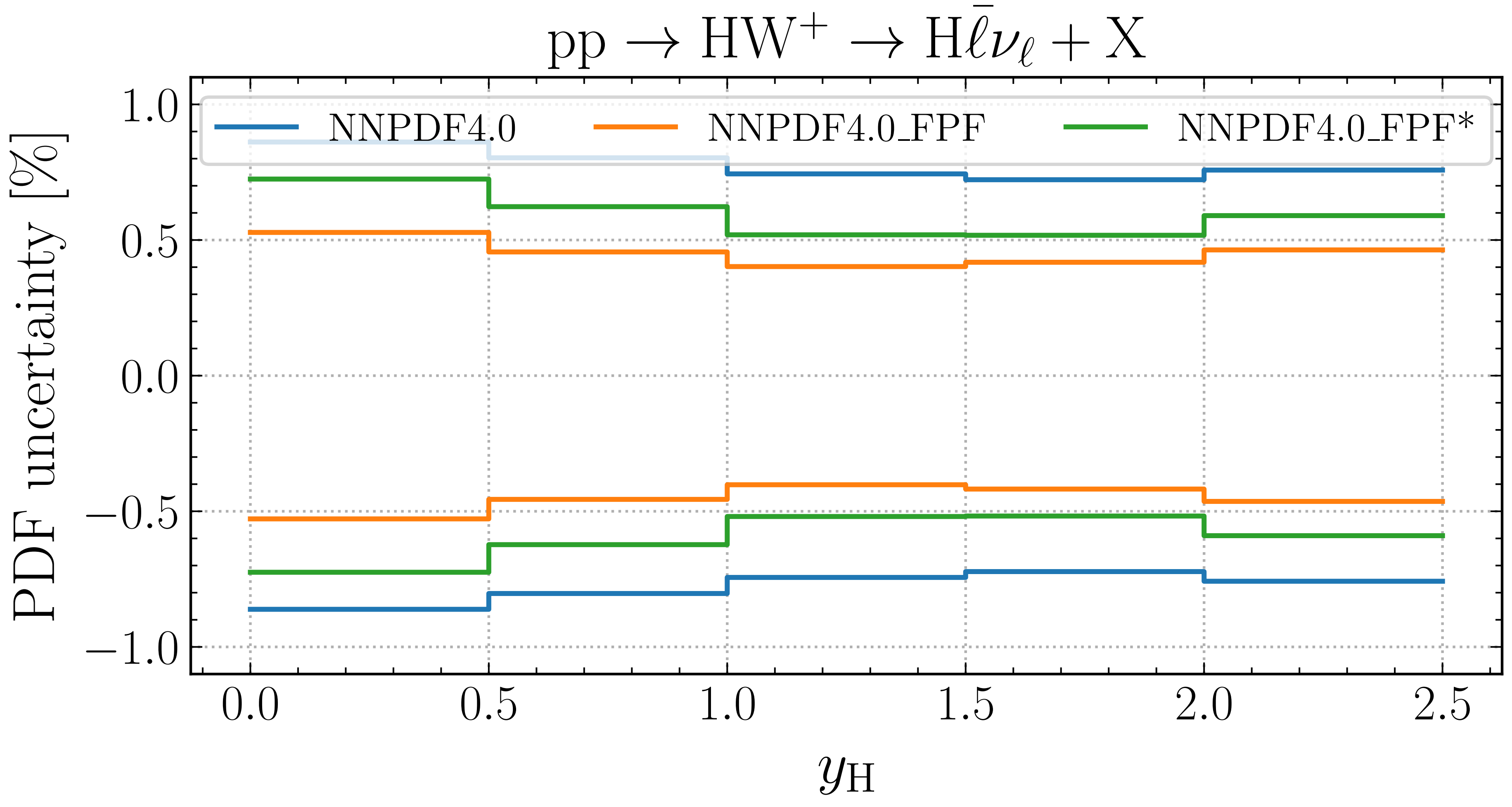

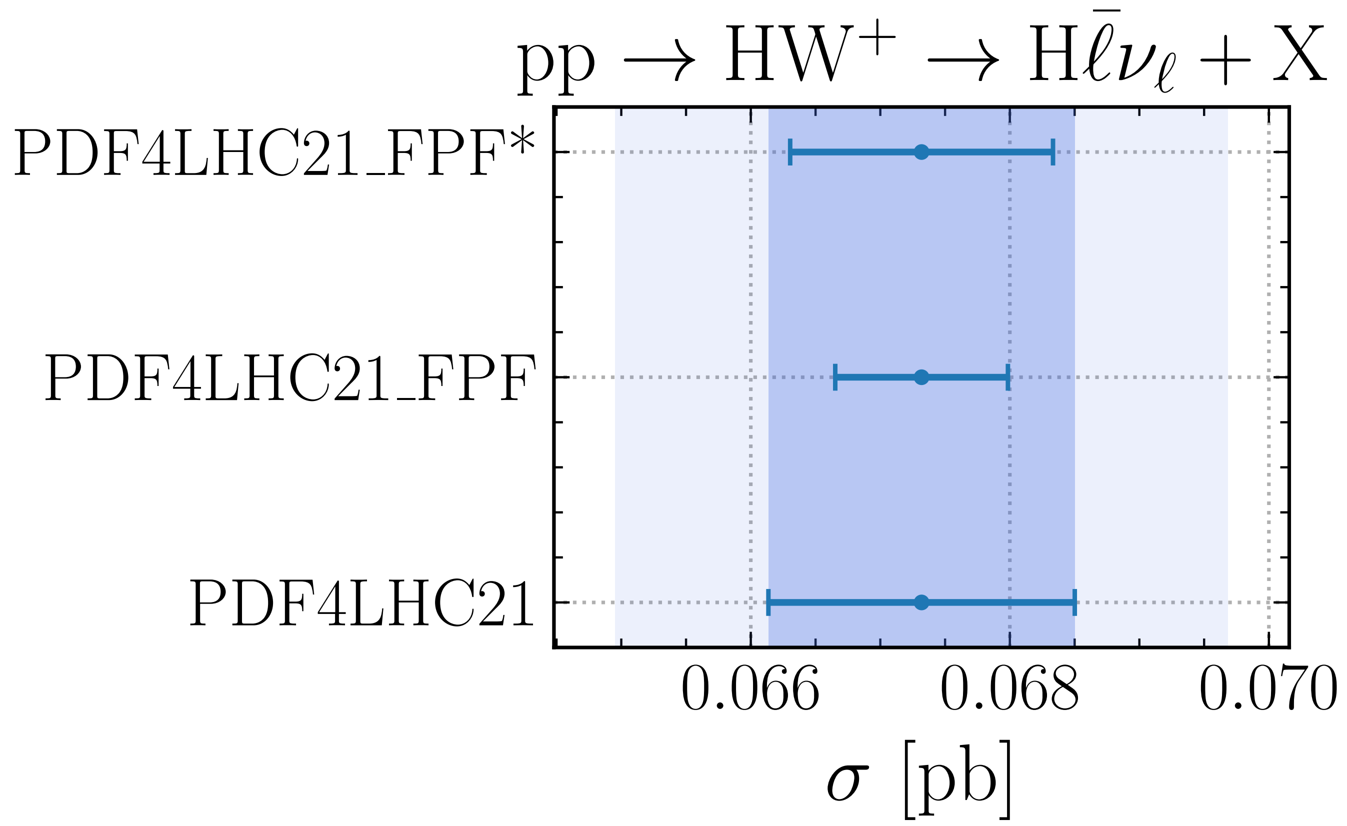

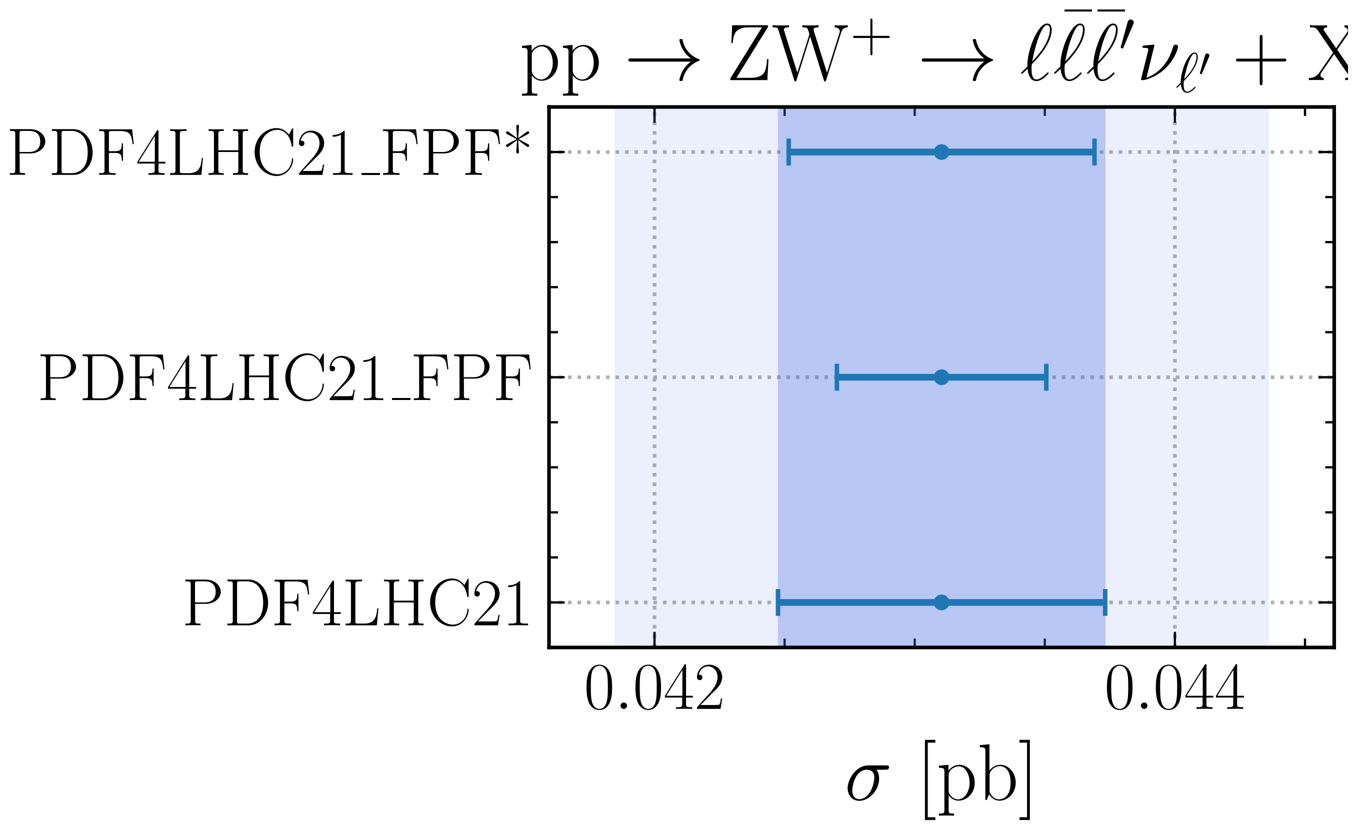

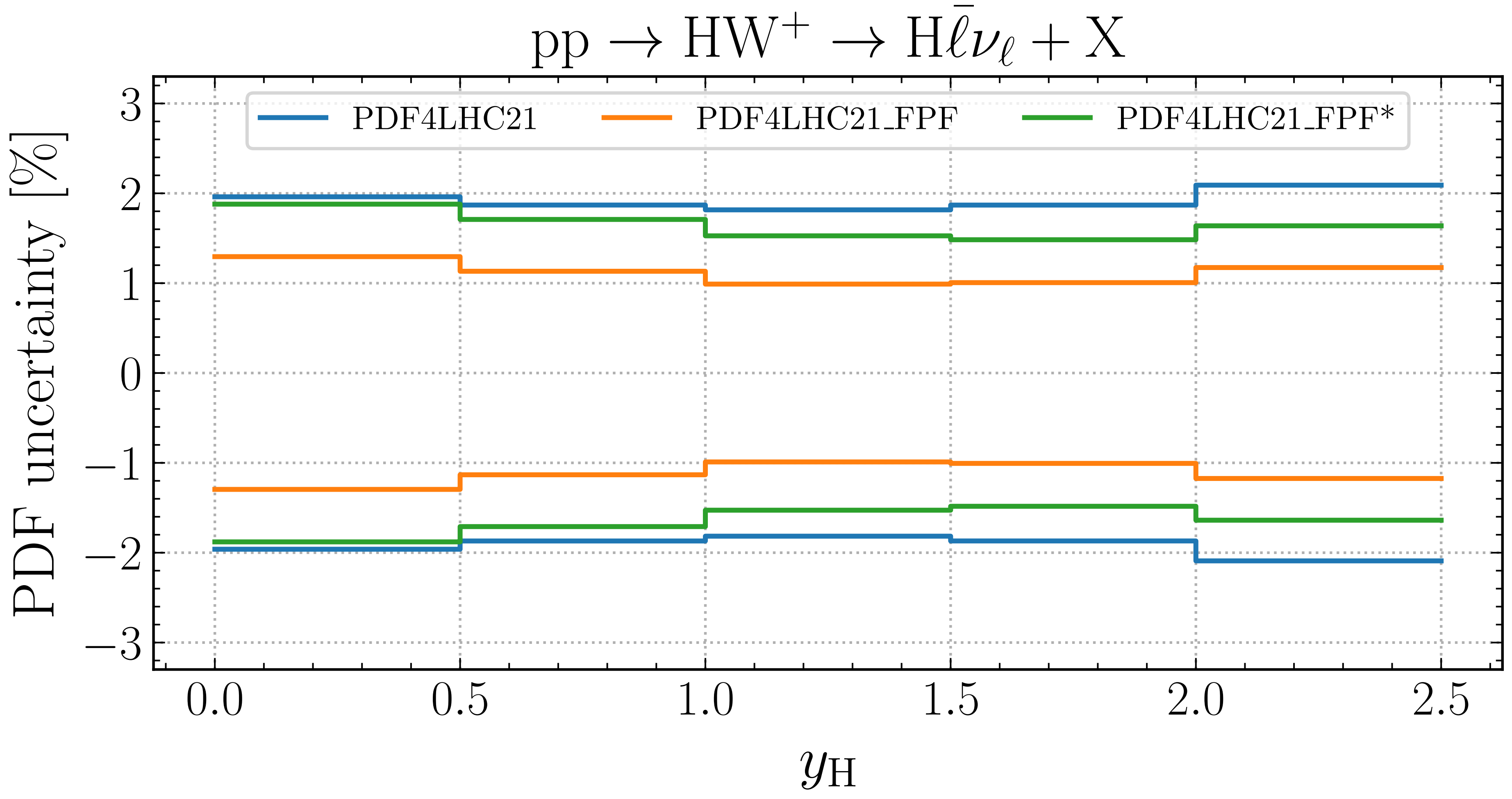

- Consistent results between the two methodologies (as was already seen at the PDF level)
- Up to a factor of 2 in the uncertainties for processes with quark-(anti)quark in the initial states

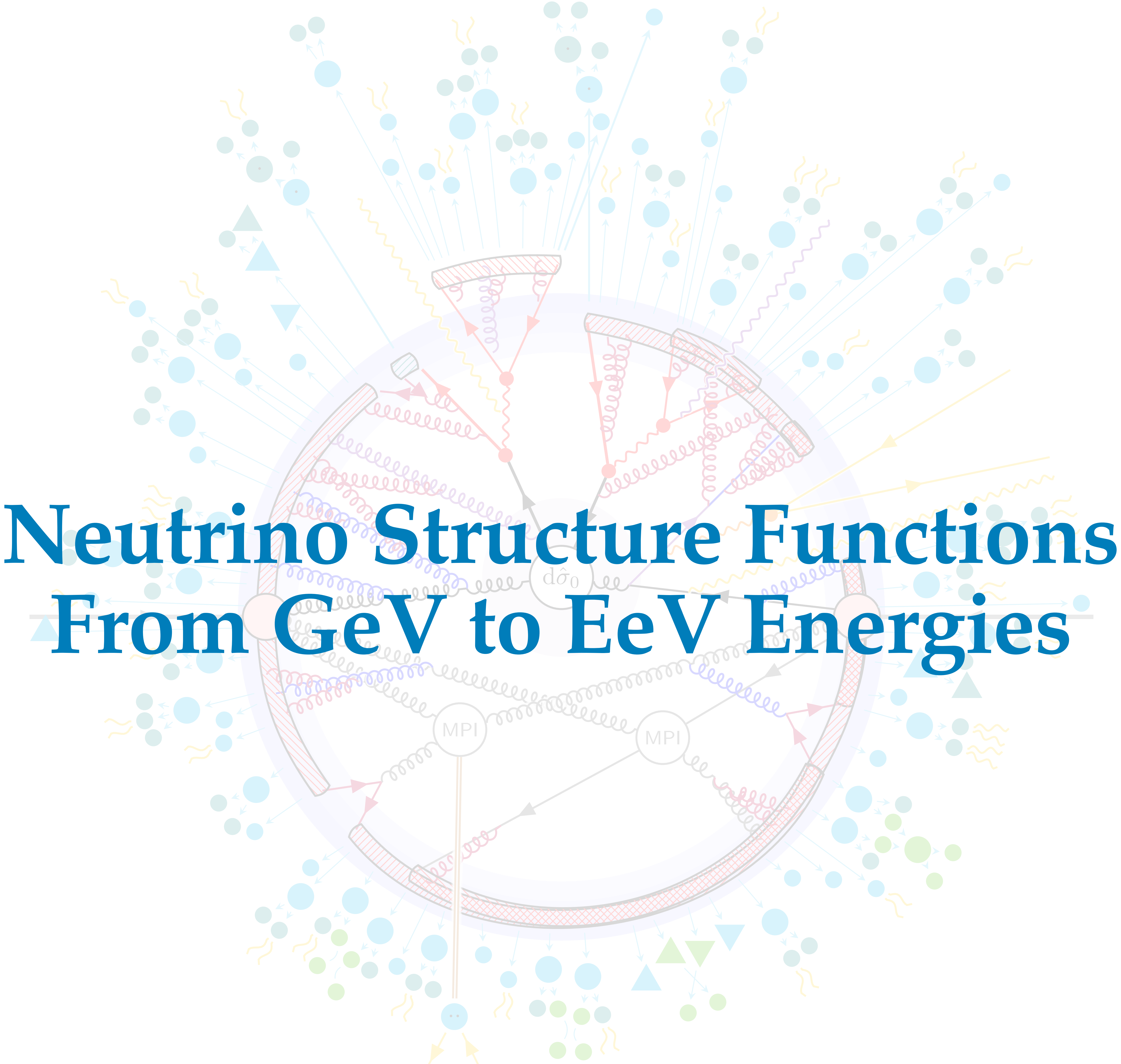

Neutrino Structure Functions From GeV to EeV Energies

[arXiv:2302.08527] In Collaboration with A. Candido, A. Garcia, G. Magni, J. Rojo, R. Stegeman

Relevance of low-Q^2 Regions in Neutrino Cross-Sections

In **muon-neutrino inelastic scattering**, at $E_\nu \sim \text{few GeV}$, the total cross-section is determined entirely by the **low-Q^2 regions:**

$$\sigma(E_\nu) = \int_{Q^2_{\text{min}}}^{2m_N E_\nu} dQ^2 \int_{Q^2/(2m_N y E_\nu)}^{1} dx \, \frac{d^2\sigma}{dx dQ^2}(x, Q^2, E_\nu)$$

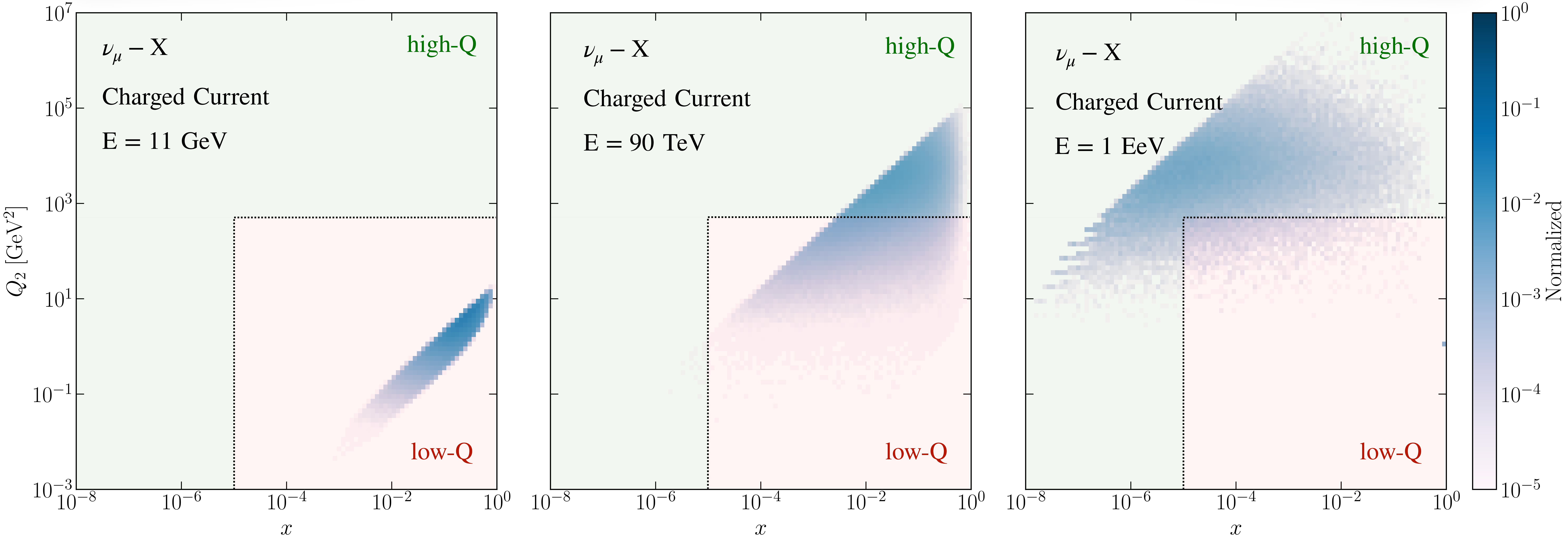

Model the low-Q^2: Bodek-Yang (BY)

BY is based on Effective LO PDFs (GRV98LO) with modified scaling variables and K-factors to approximate higher-order QCD corrections:

$$f_i^{\mathrm{LO}}(x, Q^2) \longrightarrow f_i^{\mathrm{LO}}(\xi, Q^2), \quad \text{with} \quad \xi = \frac{2x(Q^2 + m_f^2 + B)}{2Ax + \left[1 + \sqrt{1 + (2m_N x)^2/Q^2}\right]}$$

Shortcomings of the BY model:

- **Obsolete PDF parametrisation** that neglects constraints on proton & nuclear structure in the last 25 years
- **Neglect higher-order perturbative QCD calculations** (which can be significant)
- **Cannot be matched** to calculations of **high-energy neutrino scattering** based on modern PDF and higher-QCD calculations, introducing an unnecessary **separation between modelling of neutrino interactions** sensitive to **different energy regions**.
- **Lack** of **systematic estimate of the uncertainties** associated to the predictions $\iff \nexists$ **degree of belief**

Model the low-Q^2: Bodek-Yang

Bodek-Yang (BY) is based on Effective **LO PDFs** (GRV98LO) with **modified scaling variables** and **K-factors** to approximate higher-order QCD corrections:

$$f_i^{\mathrm{LO}}(x, Q^2) \longrightarrow f_i^{\mathrm{LO}}(\xi, Q^2), \quad \text{with} \quad \xi = \frac{2x(Q^2 + m_f^2 + B)}{2Ax + \left[1 + \sqrt{1 + (2m_N x)^2/Q^2}\right]}$$

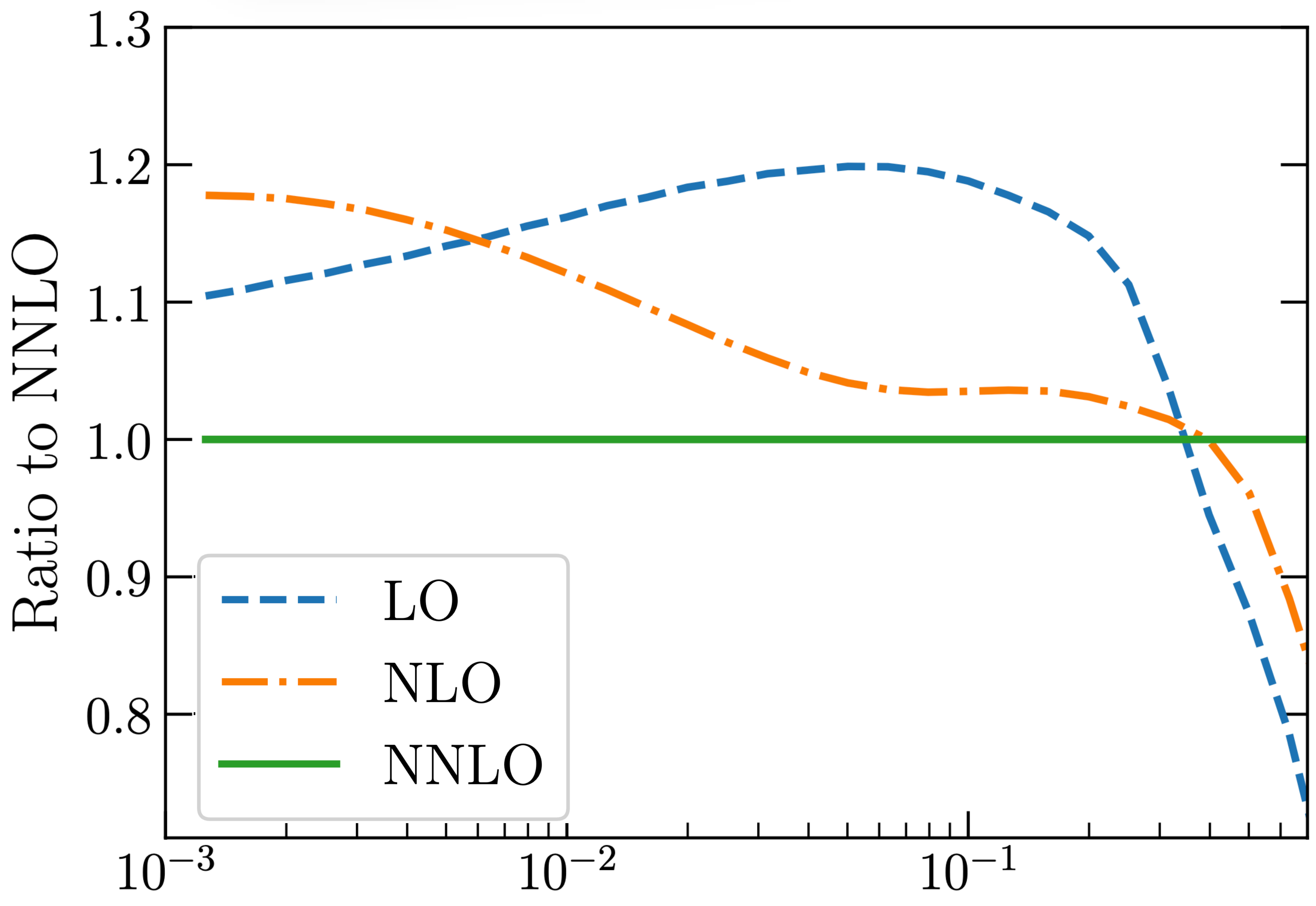

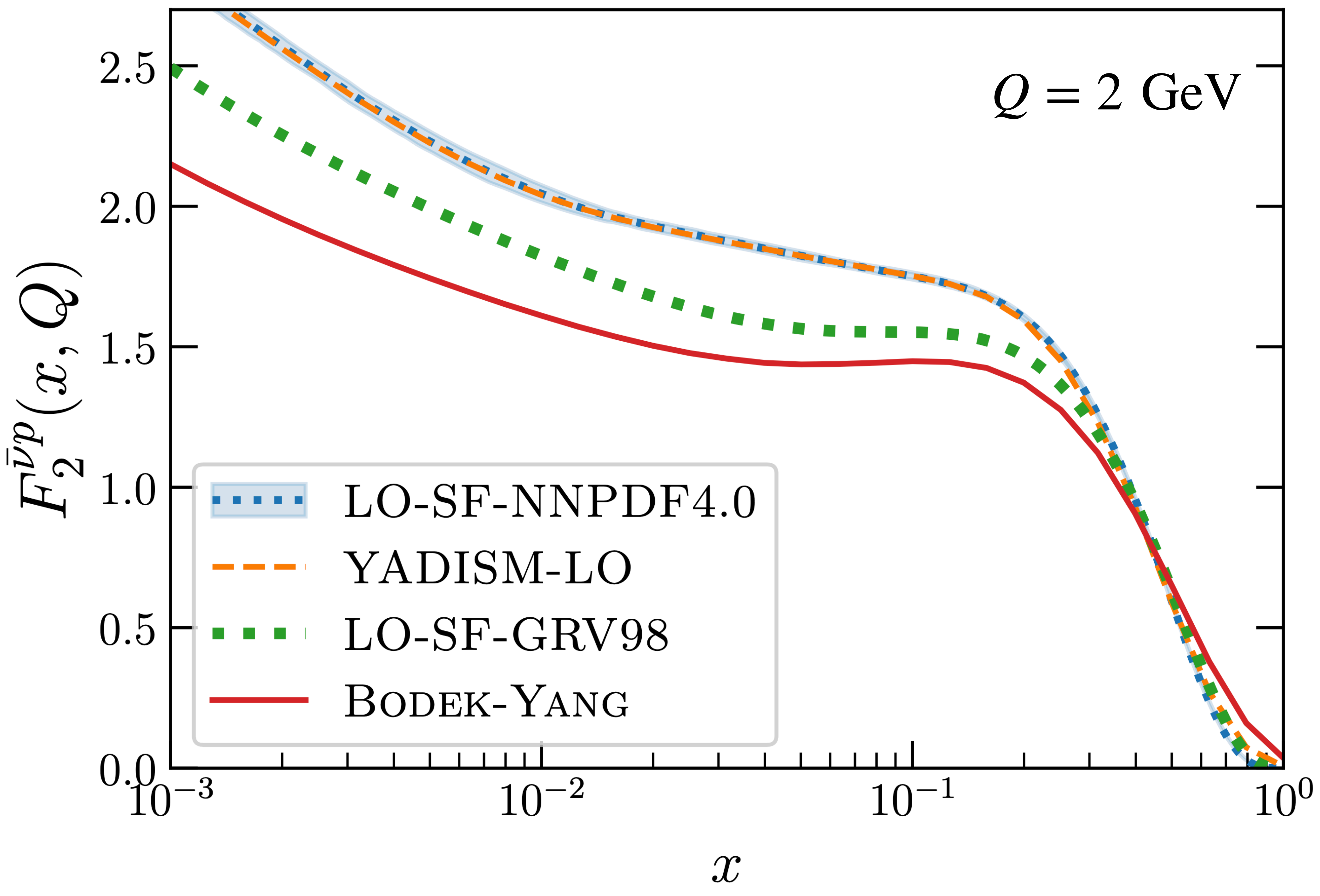

- **LO** predictions can be up to **25%** higher wrt NNLO
- **NLO** predictions can be up to **20%** higher wrt NNLO
- **BY** predictions depart from best QCD predictions even at moderate Q

NNSFν: The Approach

- Use available **data** on neutrino-nucleus scattering to **parametrise and determine the inelastic structure functions** using a NN as an unbiased interpolant
- The parametrisation is done in such a way that it **converges to the pQCD calculations at large enough Q^2**
- In the region where neutrino energy is sensitive to **large-Q^2**, the parametrisation is **replaced by pQCD calculations**

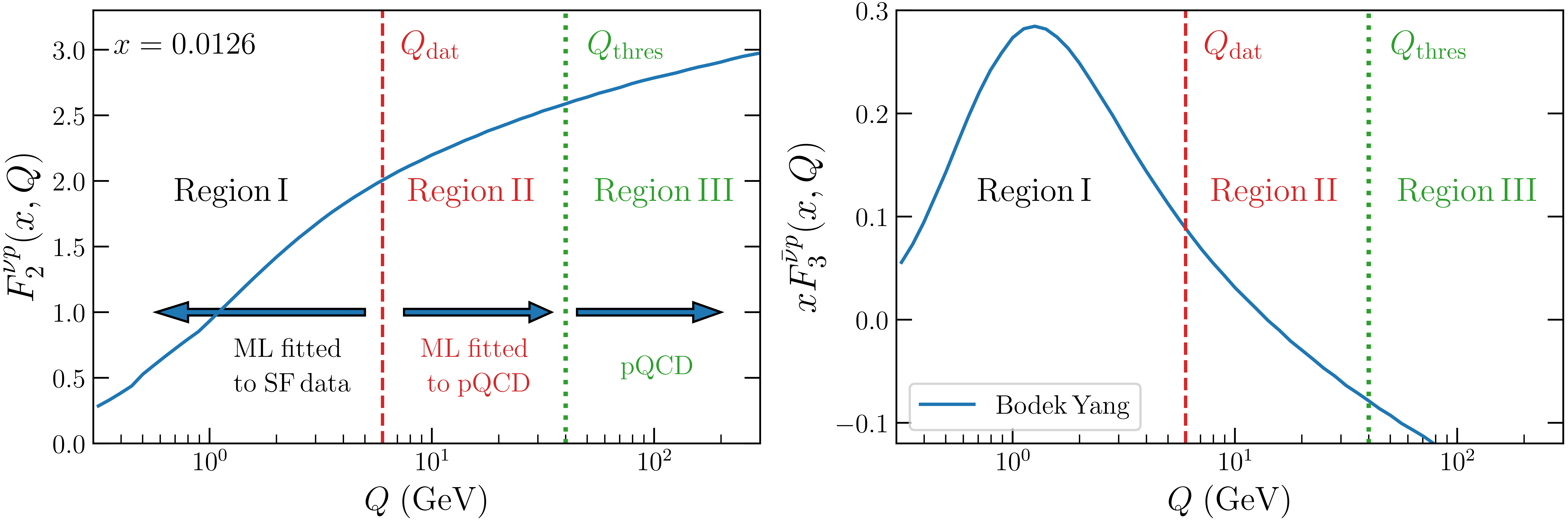

NNSFν: Experimental Inputs

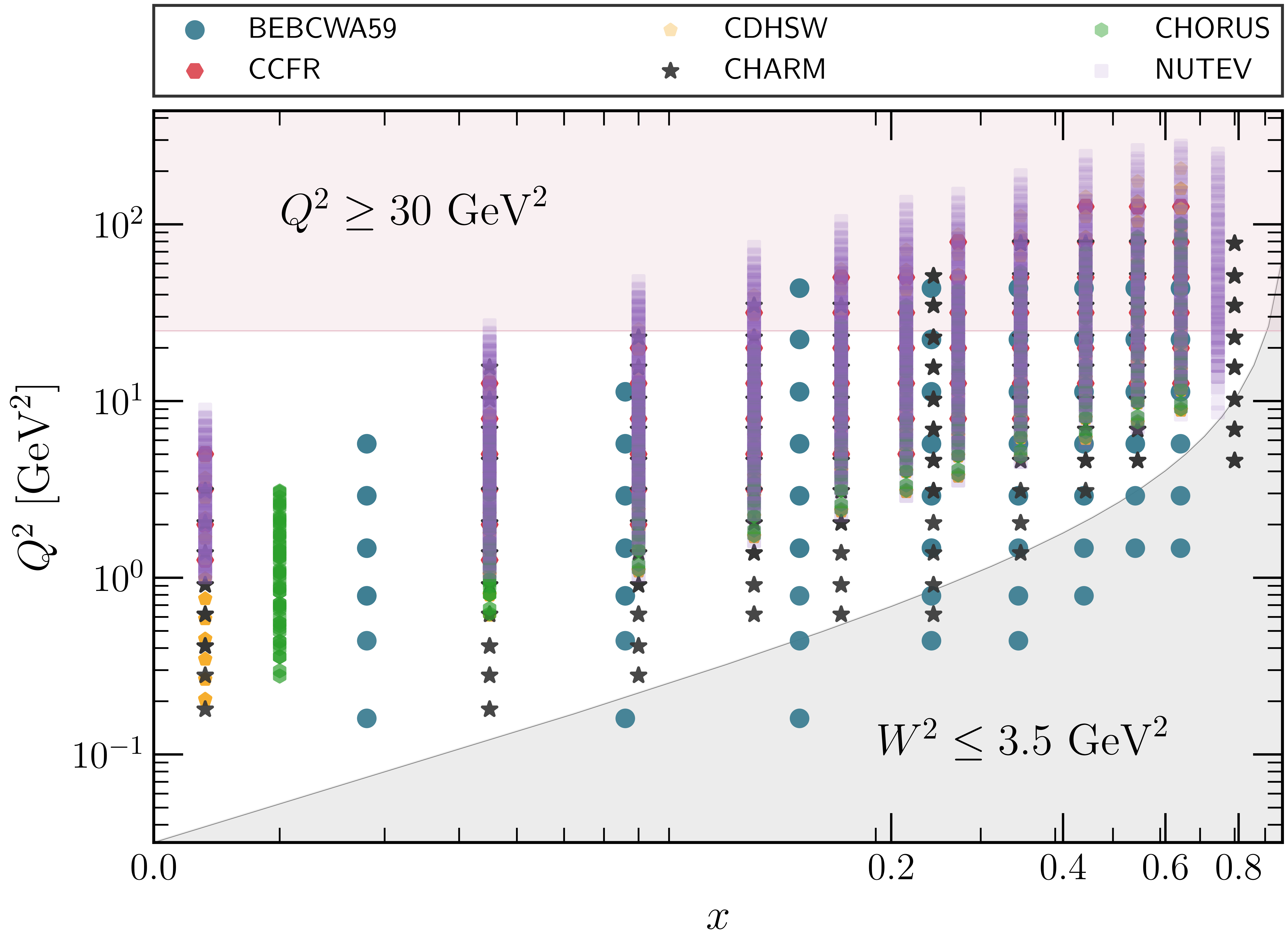

- The datasets include various **observables**, **scattering target**, and **final state** that amounts to 6224 (4184) before (after) the cut.
- The datasets span a **wide range of kinematics**. Two different types of **cuts** are applied to the experimental datasets: W^2 and Q^2_{max}.
- The resulting **determination** of neutrino inelastic structure functions are **valid for ~12 orders of magnitude in E_ν**, from ~few GeV to 10^{12} GeV.

NNSFν: Methodology

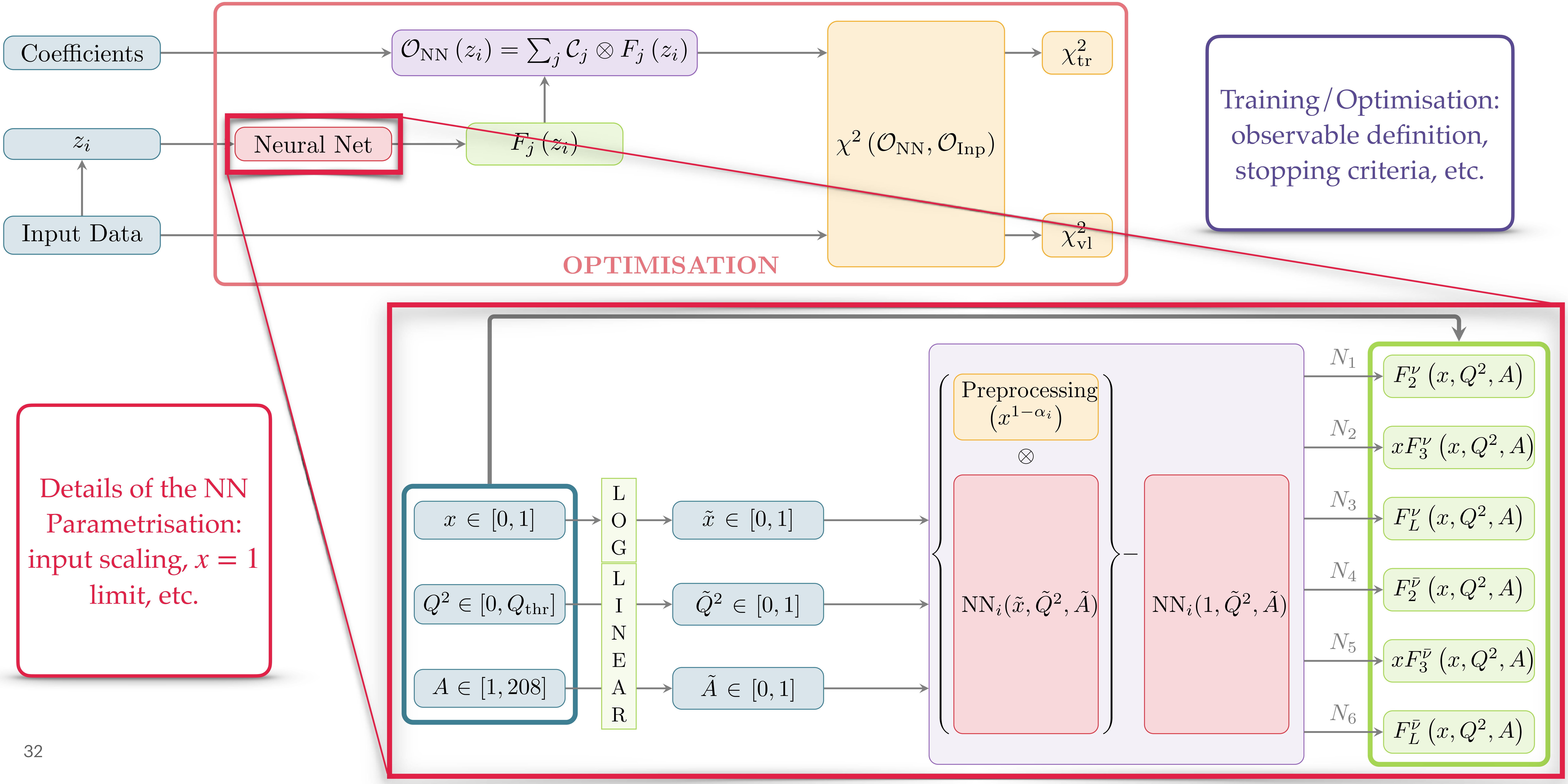

Coefficients

z_i

Input Data

Neural Net

$F_j(z_i)$

$\mathcal{O}_{\rm NN}(z_i) = \sum_j \mathcal{C}_j \otimes F_j(z_i)$

$\chi^2(\mathcal{O}_{\rm NN}, \mathcal{O}_{\rm Inp})$

$\chi^2_{\rm tr}$

$\chi^2_{\rm vl}$

OPTIMISATION

Training / Optimisation: observable definition, stopping criteria, etc.

$x \in [0,1]$

$Q^2 \in [0, Q_{\rm thr}]$

$A \in [1, 208]$

LOG

LINEAR

$\tilde{x} \in [0,1]$

$\tilde{Q}^2 \in [0,1]$

$\tilde{A} \in [0,1]$

Preprocessing $(x^{1-\alpha_i})$

$\otimes$

$\mathrm{NN}_i(\tilde{x}, \tilde{Q}^2, \tilde{A})$

$-$

$\mathrm{NN}_i(1, \tilde{Q}^2, \tilde{A})$

N_1 $F_2^\nu(x, Q^2, A)$

N_2 $xF_3^\nu(x, Q^2, A)$

N_3 $F_L^\nu(x, Q^2, A)$

N_4 $F_2^{\bar{\nu}}(x, Q^2, A)$

N_5 $xF_3^{\bar{\nu}}(x, Q^2, A)$

N_6 $F_L^{\bar{\nu}}(x, Q^2, A)$

Details of the NN Parametrisation: input scaling, $x = 1$ limit, etc.

NNSFν: Inclusive Neutrino-Nucleus Cross-Sections

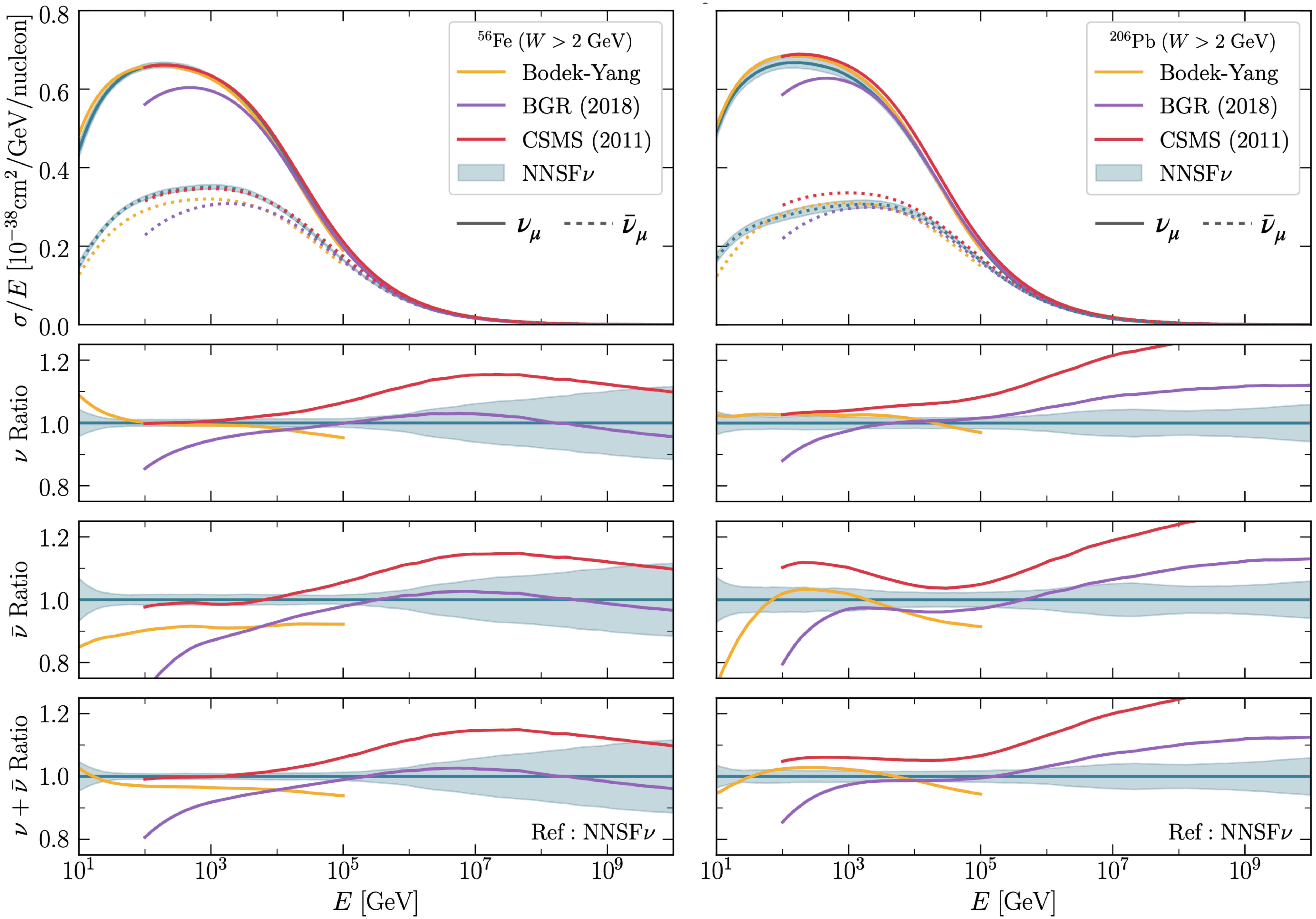

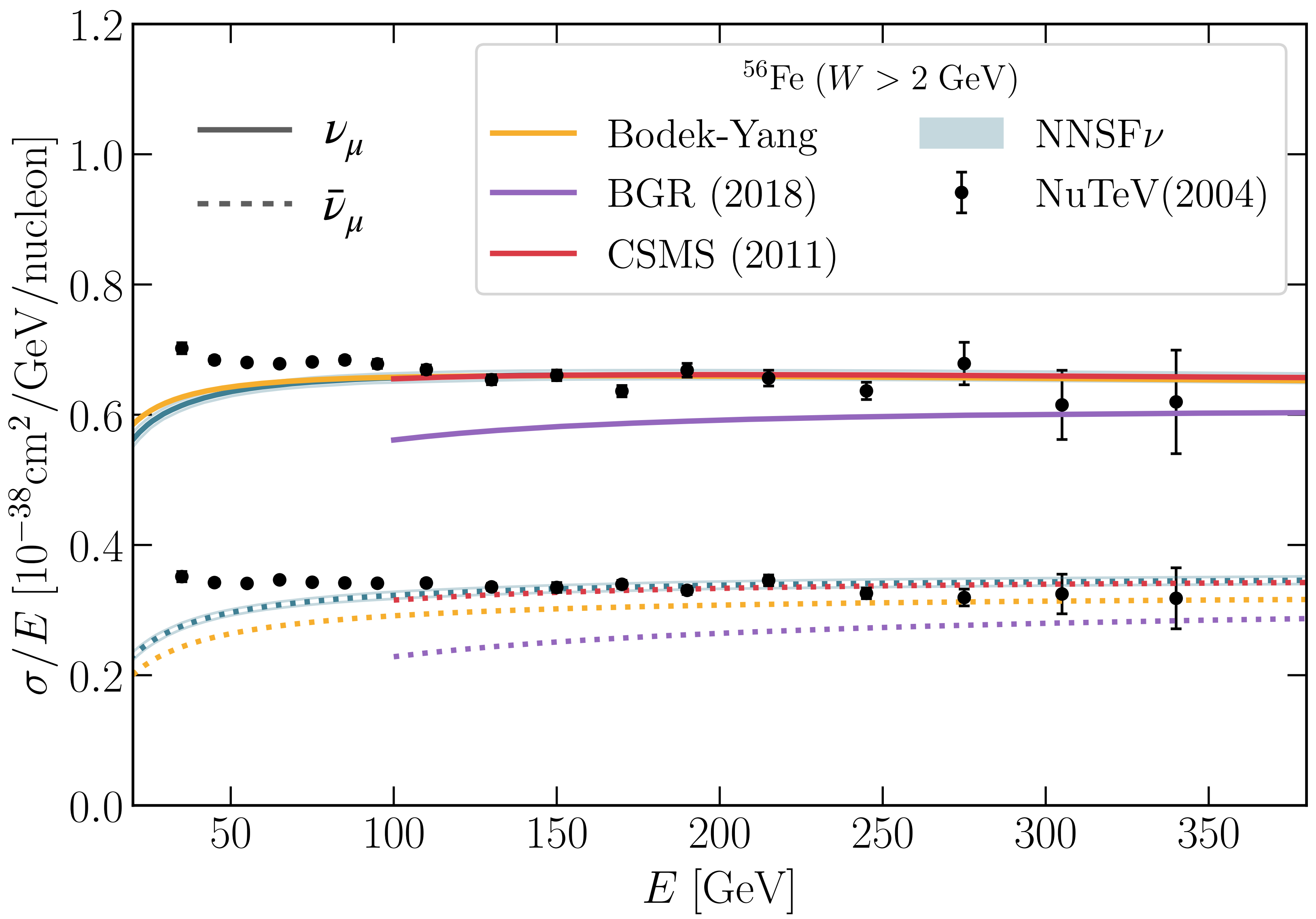

- NNSFν: only predictions **valid for all E_ν** with **uncertainty estimate**
- Reliable state-of-the-art predictions for neutrino inclusive cross-sections at **FPF energies**
- Very Good **agreement** between neutrino inelastic structure functions and cross-sections and **experimental measurements**

Conclusions and Outlook

Conclusions & Outlook

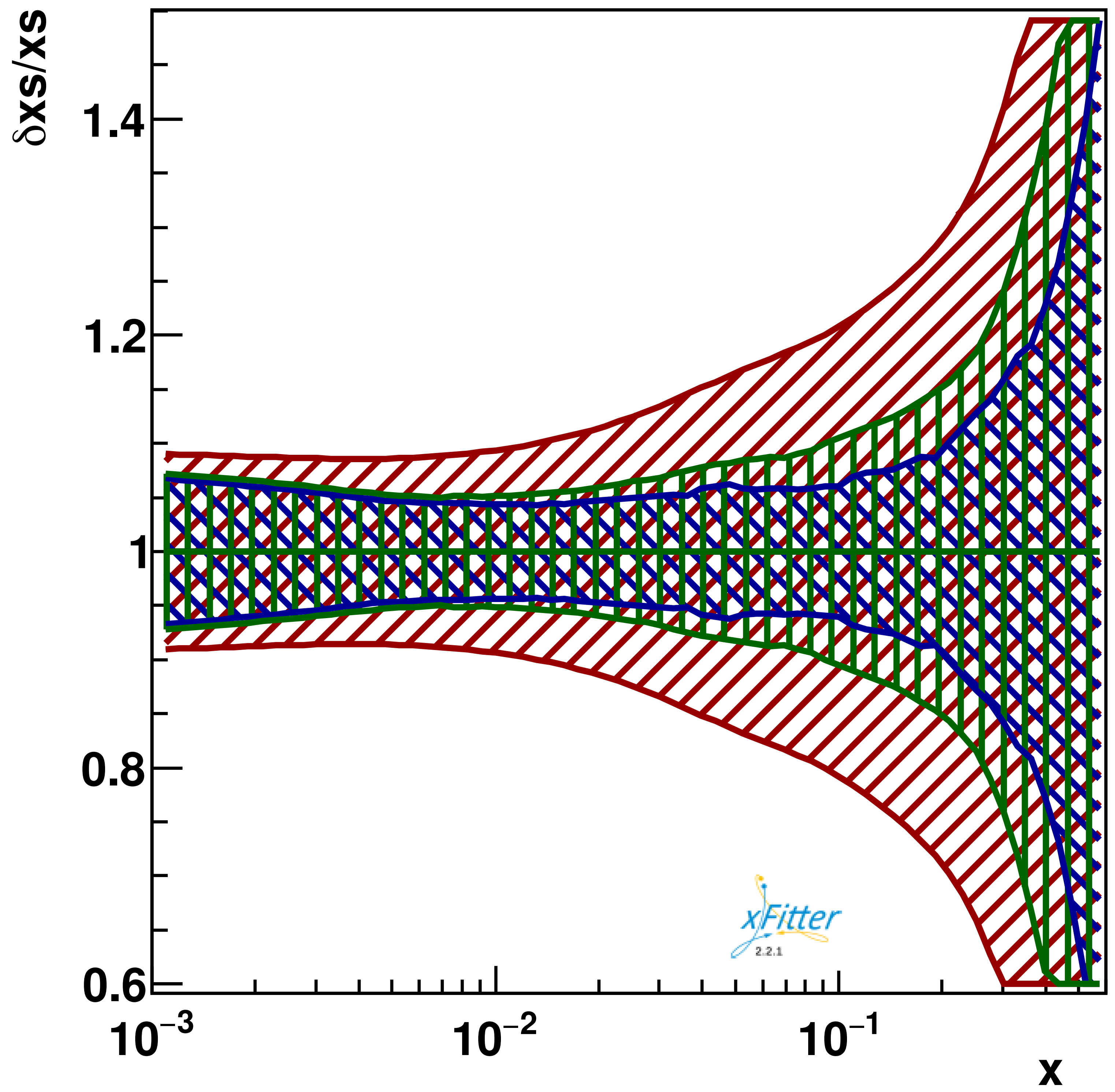

- The low-Q^2 regions contribute to a significant degree to the inclusive neutrino inelastic cross-sections
- State-of-the-art methods relying on Machine Learning provide an unbiased and better predictions for neutrino physics

- LHC neutrinos offer unprecedented opportunities to further study not only Hadron substructures but also astroparticle physics
- Measurements of neutrino DIS interactions will provide more constraints for proton and nuclear PDFs